Radiation Pattern Synthesis of Smart Fourth Dimensional (4D) Antenna Arrays Using Optimal Pulse Splitting Method

Avishek Chakraborty[1*], Ravi Shankar Saxena[2], Indrasen Singh[3], Jyoti Bansal[4], Alaa Salim Abdalrazzaq[5], Mustafa Asaad Rasol[6], Anita Gehlot[7], Sandip Bhattacharya[8], Kalyan Sundar Kola[9], Gopi Ram[10], Durbadal Mandal[11]

[1*]Department of EECE, GITAM University, Bengaluru, Karnataka, India – 561203, Tel.: (+91) 7595882913

[2]Department of ECE, GMR Institute of Technology, Rajam, Andhra Pradesh, India – 532127

[3]School of Electronics Engineering, VIT Vellore, Tamil Nadu, India – 632014

[4]Department of EEE, IES College of Technology, IES University, Bhopal, Madhya Pradesh, India

[5]Department of Dentistry, Al-Noor University College, Nineveh, Iraq

[6]College of Dentistry, National University of Science and Technology, Dhi Qar, Iraq

[7]Department ECE, Uttaranchal Institute of Technology, Uttaranchal University, Dehradun, India – 248007

[8]Department of ECE, SR University, Warangal, Telangana, India – 506371

[9]Department of ECE, SR University, Warangal, Telangana, India – 506371

[10]Department of ECE, NIT Warangal, Telangana, India – 506004

[11]Department of ECE, NIT Durgapur, West Bengal, India – 713209

[1*]achakrab3@gitam.edu, [1*]avishekdreamz@gmail.com, [2]ravishankar.s@gmrit.edu.in, [3]erindrasen@gmail.com, [4]jyoti.bansal01@outlook.com, [5]alaa.salim@alnoor.edu.iq, [6]mustafa.a.rasol@nust.edu.iq, [7]dranitagehlot@gmail.com, [8]sandip.bhattacharya@sru.edu.in, [9]kalyankola12@gmail.com, [10]gopi.ram@nitw.ac.in, [11]dmondal.ece@nitdgp.ac.in

***Corresponding author:** *Avishek Chakraborty*, **Email:** *achakrab3@gitam.edu*, *avishekdreamz@gmail.com*

Abstract – Designing and developing smart antennas with adaptive radiation characteristics is an integral part for present-day communication systems. The versatile capabilities of Time-modulated fourth-dimensional (4D) antenna arrays can provide that crucial adaptability if properly designed. This work discusses an effective analysis of 4D antenna arrays to achieve less-attenuating radiation patterns with simultaneously suppressed sidelobe and sidebands. The 4D arrays offer an additional benefit over standard arrays in the sense that the requisite amplitude tapering to lower the undesired radiations can be accomplished by controlling only the switch ON times of the radiating elements

[4]Present address: Department of ECE, Chandigarh Engineering College, Chandigarh Group of Colleges, Punjab – 140307

[9]Present address: Department of CSE, Brainware University, Kolkata, West Bengal – 700125

instead of using attenuators. The idea of splitting pulses by keeping the total switch ON durations constant, is exploited here as an additional degree of freedom for beamforming of all the radiation patterns. The unwanted radiations in terms of sidelobes as well as sideband radiations (SRs) at the fundamental and harmonic frequencies, respectively are simultaneously minimized to improve the radiation efficiencies of the 4D array. To address the conflicting aims for the synthesis of radiation patterns, a wavelet-mutation based heuristic method is also proposed. The multi-objective problem in hand is modulated in to a single objective cost function as minimization problem. The proposed outcomes are reported and compared with other state of the art works related to the same domain. Furthermore, a detailed statistical analysis is also provided to identify the strengths and weaknesses of the proposed approach.

Keywords – Beamforming, Smart antenna, Sidelobe, Sideband radiations (SRs), Time modulation.

1. Introduction

Modern communication requires smart antenna arrays with adaptive radiation characteristics. The synthesis of fourth-dimensional (4D) time-modulated antenna arrays have drawn an abundance of attention from the scientific community lately for its adaptive nature [1]. To add a further degree of control to the already existing classic antenna arrays, fourth dimension 'time' had been proposed for pattern synthesis [2]. Excitation, phase, and the distance between elements used to be the three dimensions to control the radiation pattern of traditional array. This fourth dimension provided an advantage when the idea of regulating the array patterns by rapid switches had been introduced for electronic scanning [3]. Due to its simple control by switching ON and OFF the antennas, the 4D arrays have emerged as an alternate to tapered phased arrays for achieving ultra-low sidelobe levels (SLLs) [4]. However, the benefit comes with an intrinsic limitation of sideband pattern generation at infinite number of harmonic frequencies, typically thought of as power loss [5]. So, many efforts have been made since then to synthesize adequate average patterns at antenna operating frequency to reduce the spurious harmonic or sideband radiation (SR) [6-8]. To further improve the efficiency of the array, simultaneous suppression of SLL and minimization of all higher-order sideband levels (SBLs) have been addressed [9,10]. An alternative strategy for direction finding has also emerged, one that utilizes the SBLs rather than suppressing them [11]. In addition, a novel electronic steering technique was put forth in [12] by controlling the SRs. The 4D arrays had further been investigated to estimate the directions of arrival of target signal [13] by exploiting the beamforming capabilities

of the harmonics [14]. The harmonics have also been controlled by moving the phase center of the linear 4D arrays with suitable time schemes [15,16]. Novel methods to regulate the beam patterns have been made feasible by the design of proficient switching mechanisms utilizing pulse shifting [17] and pulse splitting [18]. Pattern generation of 4D arrays by attenuating [19] or exploiting [20] the SRs has been reported for multifunction radars [21,22]. Controlling a sideband by progressive phase shifted switching [23], or multiple higher-order sidebands by optimal phase shifting [24,25] have opened up the possibilities for multipoint communication. Due to its adaptiveness, 4D arrays exhibit multifold prospect compared to its traditional counterparts if the sideband power is properly controlled [26]. Automatic beam steerable 4D arrays with single and multiple steered beams have also come into the picture by channelizing the sideband power in desired directions [27,28]. The 4D planar arrays have further been proposed for harmonic beamforming [29], and for directional modulation purposes by controlling its phase time sequences [30]. For more advanced applications like monopulse radars, sum-difference beams have also been generated using convex optimization methods [31]. Due to its efficient beamforming capabilities, 4D arrays have also been extensively investigated for physical secure communication [32,33]. Furthermore, multi-tone harmonics of 4D arrays have been explored for Wireless Information and Power Transfer (WIPT) [34]. In this way, different structures and combinations of 4D antenna array [35] with time-modulation have become a serious research interest in modern-world communication [36].

An efficient analysis of 4D linear arrays is discussed in this study in order to generate less-attenuating radiation patterns with sequentially suppressed sidelobe and sidebands. In this regard, an idea of splitting pulses while maintaining an optimal total switch ON duration is adopted as an additional level of freedom for beamforming. In order to improve the overall radiation efficiencies of the array, the SLL and SBLs at the fundamental and harmonic frequencies are minimized. A set of linear arrays containing 16, 24, and 30 elements are investigated by proposing unique splitting pulse switching sequences for each array. Pulse splitting in between an optimal modulation period provides an extra edge of control over the undesired radiations and power wasted in higher-order harmonics. The optimal pulse splitting schemes are designed by a wavelet-mutation based heuristic method by taking multiple objectives in a single-objective cost function as minimization problem. The outcomes are compared with other state of the art works, and a detailed statistical analysis is also reported to show the efficacies of the method.

The idea and methods proposed here have numerous benefits over other contemporary methods pertaining to antenna arrays employed for complex beamforming applications. The following are the key benefits in brief:

- First of all, optimal splitting pulse sequences have designed for efficient beamforming purposes.
- Second, ultra-low SLLs have been targeted by channelizing maximum power to the main beams.
- Then, unwanted SBLs have been suppressed to reduce the power wastage and improve efficiencies.
- This automatically mitigates the unwanted interferences coming from non-desired directions.
- In addition to that, all the higher sidebands are also lowered and up to 20 SBLs have been reported.
- For the overall optimization process, wavelet mutation is implemented to balance the exploration and exploitation stages. It is further compared with other hybrid and traditional mutation processes in terms of outcomes of the problem in hand.
- Finally, simultaneous mitigation of SLLs and SBLs have been proposed by implementing a single beamforming network (BFN). The proposed work is also free from BFN related implementational complexities, and provides an adaptive, robust, and efficient method of beamforming compared to the conventional ones.

The sequence of the remaining material is as follows: The design insights and the switching concept of 4D arrays are outlined in Section 2. Section 3 briefly describes a wavelet-based heuristic method. In Section 4, the results are examined with comparative and comprehensive analysis. The concluding remarks are laid out in Section 5.

2. Theory and Design Equations

The simplified beamforming network (BFN) of a 4D linear array consists of N isotropic radiators attached through rapid radio-frequency (RF) switches, is shown in Fig. 1. The corresponding array factor (AF) without any loss of generality can be given as [1]

$$AF(\theta,t) = e^{j(2\pi f_0)t} \sum_{n=1}^{N} I_n U_n(t) e^{jk(n-1)d\cos\theta} \tag{1}$$

where, I_n represents the excitation of the nth antenna, k is the propagation constant, d is considered as uniform element spacing, θ is the angle of impinging signals, f_0 is the central frequency with T_0 being the fundamental period, and $U_n(t)$ is the time modulation function.

Due to the periodic nature, $U_n(t)$ may be given as [1]

$$U_n(t) = \sum_{m=-\infty}^{\infty} a_{mn} e^{jm(2\pi f_p)t} \tag{2}$$

The Fourier term of excitation (a_{mn}) for a particular radiating antenna (n^{th}) at pre-defined harmonic frequencies (m^{th}), automatically created due to modulation, can be given as [1]

$$a_{mn} = \frac{1}{T_p} \int_0^{T_p} U_n(t) e^{-jm(2\pi f_p)t} dt \tag{3}$$

Thus, the *AF* for uniformly excited ($I_n = 1$) 4D linear array may be expressed as [9]

$$AF(\theta, t) = \sum_{m=-\infty}^{\infty} \sum_{n=1}^{N} a_{mn} \{e^{jk(n-1)d\cos\theta}\} e^{j2\pi(f_0 + mf_p)t} \tag{4}$$

The corresponding *AF* for m^{th} order frequencies may be simplified as [9]

$$AF_m(\theta, t) = e^{j2\pi(f_0 + mf_p)t} \sum_{n=1}^{N} a_{mn} e^{jk(n-1)d\cos\theta} \tag{5}$$

The central pattern is generated at $m = 0$, and SRs are placed at multiple of modulation frequencies such as $m = \pm1, \pm2, \pm3, \ldots, \pm\infty$. The directivity of the 4D array is [10]

$$Dir = \frac{|AF_0(\theta_0, \phi_0)|^2}{\frac{1}{4\pi} \sum_{m=-\infty}^{\infty} \int_0^{2\pi} \int_0^{\pi} |AF_m(\theta, \phi)|^2 \sin\theta d\theta d\phi} \tag{6}$$

where the central pattern ($m = 0$) has placed at $\theta = \theta_0, \phi = \phi_0$ in a three-dimensional plane, and $AF_m(\theta, \phi)$ denotes the *AF* pattern at m^{th} harmonics.

2.1. Basic Time Modulation Scheme

Considering its periodic character, the switching module $U_n(t)$ may be derived in different ways for different switching sequences. In order to achieve beamforming patterns, the method suggested here involves splitting and shifting of each separable pulses within a modulation period (T_p). Pulse splitting and shifted pulse, along with a general ON-OFF rectangular time scheme is shown in Fig. 2. $U_n(t)$ for the general one is expressed as [9]:

$$U_n(t) = \begin{cases} 1, 0 \le \tau_n^1 \le t \le \tau_n^2 \le T_p \\ 0, \qquad otherwise \end{cases} \tag{7}$$

The ON-time for n^{th} element is specified as τ_n within the modulation time T_p $(0 \le \tau_n \le T_p)$, and normalized ON-time is $\{\tau_n/T_p\}$. The element is turned ON initially (without shifting) as shown in Fig. 2(a) and the shifted pulse is given in Fig. 2(b). The shifted pulse starts at τ_n^1 and closes at τ_n^2 with a normalized ON-time $\{(\tau_n^2 - \tau_n^1)/T_p\}$. Taking uniform excitations $(I_n = 1)$ for each element of the array $(n = 1,2,3,\ldots N)$, a_{mn} can be determined as [9]

$$a_{mn} = \frac{1}{T_p}\int_{\tau_n^1}^{\tau_n^2} U_n(t) e^{-jm(2\pi f_p)t} dt \tag{8}$$

$$= \frac{1}{T_p}\frac{1}{\{-jm(2\pi f_p)\}}[e^{-jm(2\pi f_p)t}]_{\tau_n^1}^{\tau_n^2}$$

$$= \frac{1}{T_p}\frac{1}{\{-jm(2\pi f_p)\}}[e^{-jm(2\pi f_p)\tau_n^2} - e^{-jm(2\pi f_p)\tau_n^1}]$$

$$= \frac{1}{T_p}\frac{j}{\{m(2\pi f_p)\}}[e^{-jm(2\pi f_p)\tau_n^1}\{e^{-jm(2\pi f_p)(\tau_n^2-\tau_n^1)} - 1\}]$$

$$= \frac{1}{1/f_p}\frac{j}{\{m(2\pi f_p)\}}[e^{-jm(2\pi f_p)\tau_n^1}\{e^{-jm\pi f_p(\tau_n^2-\tau_n^1)}(e^{-jm\pi f_p(\tau_n^2-\tau_n^1)} - e^{jm\pi f_p(\tau_n^2-\tau_n^1)})\}]$$

$$= \frac{j}{2\pi m} e^{-jm(2\pi f_p)\tau_n^1} e^{-jm\pi f_p(\tau_n^2-\tau_n^1)}[-2j\sin\{m\pi f_p(\tau_n^2 - \tau_n^1)\}]$$

$$= \frac{j(-2j)}{2\pi m} e^{-jm\pi f_p(2\tau_n^1+\tau_n^2-\tau_n^1)}[\sin\{m\pi f_p(\tau_n^2 - \tau_n^1)\}]$$

$$= \frac{1}{m\pi}[\sin\{m\pi f_p(\tau_n^2 - \tau_n^1)\}]e^{-jm\pi f_p(\tau_n^1+\tau_n^2)}$$

$$= f_p(\tau_n^2 - \tau_n^1)\frac{[\sin\{m\pi f_p(\tau_n^2 - \tau_n^1)\}]}{[m\pi f_p(\tau_n^2 - \tau_n^1)]} e^{-jm\pi f_p(\tau_n^1+\tau_n^2)}$$

$$= \frac{(\tau_n^2 - \tau_n^1)}{T_p}[\sin c\{m\pi f_p(\tau_n^2 - \tau_n^1)\}]e^{-jm\pi f_p(\tau_n^1+\tau_n^2)} \tag{9}$$

Equation (9) represents the pulse shifted scheme of Fig. 2(b).

2.2. Switching with Splitting Pulses

To address a wide range of purposes, various switching mechanisms may be devised. Towards this purpose, a sub-sectioned splitting pulse scheme for n^{th} element is given in Fig. 2(c), where the ON-time of each antenna is split up into sub-sections having an OFF-time in between. The n^{th} element is turned ON at τ_n^1 ($\tau_n^1 = 0$) and stays ON up to τ_n^2 creating an ON-duration of τ_{n1} ($= \tau_n^2 - \tau_n^1$). Then, the antenna is turned OFF and stays OFF from τ_n^2 to τ_n^3 before going into the ON-state again for a duration of τ_{n2} ($= \tau_n^4 - \tau_n^3$). The modulation function $U_n(t)$ of the sub-pulse can be given as

$$U_n(t) = \begin{cases} 1, \tau_n^1 \le t \le \tau_n^2 \le T_p, & where \quad \tau_n^1 = 0 \\ 1, \tau_n^3 \le t \le \tau_n^4 \le T_p, & where \quad \tau_n^1 \le \tau_n^3 \\ 0, & otherwise \end{cases} \tag{10}$$

The a_{mn} for the sub-sectioned pulses may be expressed as

$$a_{mn} = \frac{(\tau_n^2 - \tau_n^1)}{T_p}[\sin c\{m\pi f_p(\tau_n^2 - \tau_n^1)\}]e^{-jm\pi f_p(\tau_n^1 + \tau_n^2)} + \frac{(\tau_n^4 - \tau_n^3)}{T_p}[\sin c\{m\pi f_p(\tau_n^4 - \tau_n^3)\}]e^{-jm\pi f_p(\tau_n^3 + \tau_n^4)} \tag{11}$$

These derivations indicate that modified switching schemes offer higher degrees of freedom (DoF) than the standard ON-OFF sequence. This added DoF can be effectively utilized by manipulating the harmonics without altering the central beam pattern. Splitting each time period into multiple time steps with different switch-ON instants, optimized switch-ON and switch-OFF intervals can be summarized from equation (11) as follows:

$$a_{mn}^r = \sum_{r=1}^{s} \frac{(\tau_n^{r+1} - \tau_n^r)}{T_p}[\sin c\{m\pi f_p(\tau_n^{r+1} - \tau_n^r)\}]e^{-jm\pi f_p(\tau_n^r + \tau_n^{r+1})} \tag{12}$$

Equation (12) represents splitting pulse shown in Fig. 2(c). Here, $r = 1$ represents only the shifting of pulses for each antenna, and $r > 1$ can be accounted for splitting of pulses into sub sections and shifting them with optimal time intervals between each sub-sectioned pulse. By taking $r = 0$, the generalized expression of a_{mn} for the mth harmonic at $m = 0$ can also be found from eqn. (12) as:

$$a_{mn} = \frac{\tau_n}{T_p}\{\sin c(m\pi f_p \tau_n\}e^{-jm\pi f_p(\tau_n)} \tag{13}$$

where, $\tau_n = (\tau_n^2 - \tau_n^1)$ and the excitation coefficient of central pattern ($m = 0$) is given as: $a_{mn} = \{\tau_n/T_p\}$. This indicates that the central beam is not altered with splitting and shifted pulse, as it is mathematically related only to the switch-ON time of the antennas. But the SR patterns depend on switch-ON instants as well as the switch-ON time periods for beamforming.

2.3. Design Equation for Optimization

Therefore, it turns out that the sideband power losses can be suppressed by properly adjusting the values of the static excitations, as well as the durations and starting instants of the ON-time pulses. To further reduce the optimization burden and the control parameters, uniform amplitude is taken in to account. Then, using an iterative heuristic optimization approach, the switch-ON instants and the switch-ON time periods are tuned with the goal of minimizing the SLLs and SBLs of a specific cost function. Reduction in sideband power losses and interference rejection of the central pattern for beamforming may be targeted as a minimization problem. By optimizing the normalized ON-time periods of each antenna, the SLL of the main beam can be lowered. Sideband radiation power may be is averaged over the whole angular region by optimally shifting and splitting the ON-time pulses. The CF for the overall optimization process is designed as

$$CF = \{\Psi^{SLL(i)}(\tau_n)\}|_{f_0 \pm mf_p\,(m=0)} + \{\Psi^{SBL(i)}(\tau_n, \tau_r)\}|_{f_0 \pm mf_p\,(m=1,2,3,\ldots,\infty)} \quad (14)$$

where, $\psi^{\mathrm{SLL}(i)} = \mathrm{H}[\mathrm{SLL_{REF}} - \mathrm{SLL_{OBS}}](|\mathrm{SLL_{REF}} - \mathrm{SLL_{OBS}}|^2/|\mathrm{SLL_{REF}}|^2)$, $\mathrm{SLL_{REF}}$ and $\mathrm{SLL_{OBS}}$ are the reference and observed SLLs respectively, $\psi^{SBL(i)}$ represents the minimization of all the higher SBLs, H[.] is the Heaviside unit step function, and i denotes the number of evolutions performed for the optimization process.

3. Heuristic Optimization Technique

Heuristic optimization algorithms are robust and adaptive in nature, and combines the exploration and exploitation strategies to investigate a solution space for optimum solutions [37]. Evolutionary optimizations have evolved as population-based metaheuristic search method motivated by natural phenomena for solving various real-world engineering problems, especially in the area of antenna array synthesis [38-40].

3.1. Standard Particle Swarm Optimization

Particle swarm optimization (PSO) is a well-known, robust, and stochastic optimization tool based on the movement and intelligence of swarms [41]. Standard PSO (SPSO) has been demonstrated to be beneficial for a number of fields for optimizing challenging multidimensional discontinuous problems especially antenna design and pattern synthesis in electromagnetics [41]. SPSO models the sociological behaviour of bird flocking and fish schooling in multi-dimensional space. It takes into account a number of particles that collectively constitute a swarm. Each particle in the swarm traverses the solution space looking for the global best (g_{best}) while considering their individual or personal best (p_{best}) also at each iteration. The process continues by minimizing the distance between the present position of the particle and its personal best (p_{best}), as well as, the distance between the present position of a particle and the global best (g_{best}) as per the following equations:

$$v_j^p(i+1) = C_F.\{w.v_j^p(i) + \varphi_1.rand_1.(p_{best\,j}^{\ p} - s_j^p(i)) + \varphi_2.rand_2.(g_{best\,j} - s_j^p(i))\} \tag{15}$$

$$s_j^p(i+1) = s_j^p(i) + v_j^p(i+1) \tag{16}$$

Here, eqn. (15) and (16) are the velocity updating and position updating equations, respectively. The $v_j^p(i)$ is the velocity at i[th] iteration, with $p = 1,2,\dots,\gamma$ being the number of particles in the swarm and $j = 1,2,\dots,\kappa$ being the dimension of the particle. The φ_1 and φ_2 in eqn. (15) represents the social and cognitive acceleration constants; w is the inertia weight factor; $s_j^p(i)$ is the present position of a particle in the search space; $rand_1$ and $rand_2$ are the random numbers in between 0 and 1. The C_F stands for the constriction factor which affects the stability analysis by ensuring no premature convergence, and mathematically represented in terms of acceleration constants as [42]:

$$C_F = \frac{2}{|\,2-\varphi-\sqrt{(\varphi^2-4\varphi)}\,|} \tag{17}$$

Here, $\varphi = \varphi_1 + \varphi_2$ and $\varphi > 4$.

3.2. Hybrid PSO with Wavelet Mutation

Towards the near-optimal solution, SPSO typically encounters issues related to velocity updating despite working effectively in the beginning. If the particle's present state is coinciding with global best position, the particle will only move from its present state if its inertia weight and velocity are different from zero. The particles will stop moving if their velocities are near to zero, and they will

catch up with the g_{best}, which may result in an early convergence and prevent future development by being stagnant at a particular position. To balance the global and local explorations, the inertia weight factor w may be chosen dynamically as [42]:

$$w = \left[w_{\max} - \{ (\frac{w_{\max} - w_{\min}}{i_{\max}}) * i \} \right] \tag{18}$$

Here, i_{max} presents the maximum iterations; and w is varied between the upper (w_{max}) and lower (w_{min}) limits in a range of [1,0.4]. The hybrid PSO (HPSO) is proposed by integrating the mutation operation of genetic algorithms [43] to break through the stagnation stages of SPSO as following:

$$mut(s_j) = \begin{cases} (s_j - k), r < 0 \\ (s_j + k), r \geq 0 \end{cases} \tag{19}$$

Here, s_j is the randomly chosen element of the particle from the swarm; r is a random number in between –1 and 1; k is randomly generated within [0,0.1 $*$ ($par_{max}^j - par_{min}^j$)]; where par_{min}^j and par_{max}^j are the lower and upper limits of each particle, respectively. However, the mutation space in HPSO is limited by k. It might not be the best approach to always fix the size of the mutation space during the search. Rather, a dynamic mutation process that dynamically shrinks the mutation space along the search may be integrated. To implement this, a wavelet mutation (WM) approach is integrated with HPSO.

3.2.1. Basic Wavelet Theory

The translating and dilating oscillatory properties of some specific seismic signal may be modelled in to a continuous function $\psi(x)$ generally called as '*Morlet*' or '*mother wavelet*' if it satisfies the following properties [42]:

Property 1: $\int_{-\infty}^{+\infty} \Psi(x) dx = 0$ (20)

Property 2: $\int_{-\infty}^{+\infty} |\Psi(x)|^2 < \infty$ (21)

It means that the total momentum of $\psi(x)$ is equal to zero, or the positive and negative momentum of $\psi(x)$ is equal to each other. Also, the continuous function $\psi(x)$ can be said finite and bounded. A typical '*Morlet wavelet*' is shown in Fig. 3(a), and may be represented mathematically as [42]

$$\Psi(x) = e^{-x^2/2} cos(5x) \tag{22}$$

For controlling the magnitude and position of the '*Morlet wavelet*', the continuous function $\psi(x)$ is extended as [42]

$$\Psi_{ab}(x) = \frac{1}{\sqrt{a}} \Psi\left(\frac{x-b}{a}\right) \tag{23}$$

Here, a and b are the dilating and translating parameters, respectively. With $b = 0$, the amplitude scaled version of $\psi(x)$ can be derived. The scaled $\psi_{a,0}(x)$ for the different dilation properties are shown in Fig. 3(b), and can be represented mathematically as [42]

$$\Psi_{a,0}(x) = \frac{1}{\sqrt{a}} \Psi\left(\frac{x}{a}\right) \tag{24}$$

The amplitude can be scaled down by increasing the value of dilating parameter, and this property is utilized in the mutation process to enhance the search performance of the algorithm [42].

3.2.2. Operation of the WM

The wavelet-based mutation exhibits fine tuning by giving every element particle of the swarm a chance to mutate within a user-defined mutation probability $P_m \in [0,1]$. Thus, if the p^{th} particle is chosen and the element particle of the swarm $x_j^p(i)$ is selected randomly for mutation, the resultant particle can be given as [42]

$$\overline{x_j^P}(i) = \begin{cases} x_j^P(i) + \sigma.[par_{\max}^j - x_j^P(i)] & if\ \sigma < 0 \\ x_j^P(i) + \sigma.[x_j^P(i) - par_{\min}^j] & if\ \sigma < 0 \end{cases} \tag{25}$$

Here, $\sigma = \psi_{a,0}(x) = \frac{1}{\sqrt{a}}\psi\left(\frac{x}{a}\right)$ and $\psi(x) = e^{\left(-\frac{x^2}{2}\right)} cos(5x)$. So, dilating parameter (σ) becomes

$$\sigma = \frac{1}{\sqrt{a}} e^{\left\{\frac{\left(-\frac{x}{a}\right)^2}{2}\right\}} cos\left\{5\left(\frac{x}{a}\right)\right\} \tag{26}$$

When σ is positive ($\sigma > 0$) and approaching to +1, the mutated particle element tends to have the maximum of $x_j^p(i)$. On the other hand, when σ is negative ($\sigma \leq 0$) and approaching to –1, it has the minimum value of $x_j^p(i)$. The larger the value of $|\sigma|$, the searching space for fine tuning is large and vice-versa. According to the properties of mother wavelet, the sum of the positive and negative σ are equal when the sample is large. Thus, the positive and negative mutation is equal which provides a better solution stability. Further, the dilating parameter (a) can be expressed as

$$a = e^{-ln(g)*\left(1-\frac{i}{k}\right)^{\xi_{wm}}+ln(g)} \tag{27}$$

The dilating parameter (a) varies with $\left(\frac{i}{K}\right)$, where i stands for current evolution and K is the total number of evolutions. The monotonically increasing shape parameter is denoted by ξ_{wm} and g is the upper limit of the dilating parameter a [1,10000]. In HPSOWM, an optimal balance is projected between the exploitation of previously sampled regions in the search space and the exploration of new regions. An updated swarm is created after the WM operation, and the swarm will follow the same process over and over again until the termination criteria is reached.

4. Numerical Data and Analysis

This upcoming section discusses the numerical outcomes by a thorough examination of 16, 24, 30-element 4D linear arrays that have been developed, where the required objectives are achieved by combining a soft computing method with pulse control methodologies. The operational frequency (f_0) of the 4D linear arrays is 3 GHz with a modulation frequency (f_p) of 1 MHz. The properties of isophoric (I_n = 1) 16, 24, 30-element 4D linear arrays are: Peak SLLs = –13.15 dB, –13.21 dB, –13.24 dB; 3 dB beamwidths (HPBWs) = 6.48˚, 4.32˚, 3.60˚; beamwidth within the first nulls (FNBWs) = 14.4˚, 9.72˚, 7.56˚; and directivities = 12.04 dB, 13.80 dB, 14.77 dB; respectively. All the simulations are performed with MATLAB.

4.1. Beamforming with Splitting Pulses

An analysis of 4D linear arrays is investigated here in order to produce less-attenuating radiating beam patterns with sequentially lowered SLLs and SBLs. First, high-directive beamforming arrays with ultra-low SLLs are targeted, and then all the higher SBLs are minimized to reduce unwanted power loss. The aim is to design the optimal switching schemes by splitting the pulses within the pre-specified modulation period such that the SLL and the SBLs can be minimized to reduce the unwanted interference and the undesired power radiation in higher harmonics, respectively. The possible application of beamforming array is for directive point-to-point communication systems.

4.1.1. Beamforming with 16-Element Array

The 16-element beamforming 4D linear array is developed by aiming the objective of simultaneous SLL and SBLs reduction using pulse splitting. The ON-time and the pulse splitting instants of each array element are optimized, along with the uniform distance between each of them. The optimal outcomes are targeted by the proposed HPSOWM algorithm. The HPSOWM-based outcomes are also compared with HPSO and SPSO-based outcomes. To minimize the SBLs, the optimized ON-times of each antenna splits in two halves and shifted, so that the unwanted SRs can be outspread in a uniform way. The ON-times of the first pulse and the splitting instants of the second pulse are taken into account for optimization. Pulse splitting and shifting do not affect the central pattern, as central beam depends only upon the ON-time period. Thus, the central beam kept unchanged. The optimized beamforming switch schemes without and with pulse splitting derived by HPSOWM are presented in Fig. 4 (a) and (b). The radiation pattern for point-to-point beamforming array is given in Fig. 5. Here, the uniform pattern, as well as the optimized main beam pattern (f_0 at m = 0) with isotropic and directive elements are shown. The fixed inter-element spacing between each antenna is kept as 0.75λ. The radiation patterns obtained with HPSO and SPSO are also presented in Fig. 6 (a) and (b), respectively. The proposed HPSOWM-based array is reported with a reduced PSLL of –40.48 dB compared to –13.15 dB PSLL of isophoric 4D array. HPSOWM-based pulse splitting approach also produces low SBLs, and the first two SBLs are reported as –42.6 dB and –48.38 dB. The FNBW and directivity reported for the proposed 4D array are 17.64º and 12.98 dB compared to 14.4º and 12.04 dB of isophoric array, respectively. The WM method is superior over the HPSO and SPSO methods as –37.81 dB and –33.89 dB PSLLs are obtained against –42.6 dB. The power at sideband is directly proportional to the nature of higher-order SBLs. The power generated at the main beam and first ten higher-order harmonics is shown in Fig. 7 (a). In addition

to that, the first twenty higher SBLs are also reported in Fig. 7 (b) shows that the target objective of SLL and SBLs reduction are achieved simultaneously with the proposed 4D arrays. In the proposed beamforming array with HPSOWM, 70.61% power is utilized and 29.39% is wasted in higher-order harmonics compared to 70.01%, 29.99% and 68.72%, 31.28% obtained with HPSO and SPSO, respectively. The optimized numerical outcomes are shown in Table 1. The possible application of the proposed work is high-directive point-to-point communication system.

4.1.2. Beamforming with 24-Element Array

The 24-element beamforming 4D linear array is proposed here by aiming SLL and SBLs reduction simultaneously through pulse splitting. The ON-time and the pulse splitting instants of each array element are optimized. The optimal results are targeted by HPSOWM algorithm. The HPSOWM-based results are then compared with HPSO-based, SPSO-based and uniform 4D linear arrays. The optimized beamforming switch schemes without and with pulse splitting derived by HPSOWM are presented in Fig. 8 (a) and (b). The radiation pattern for point-to-point beamforming array is given in Fig. 9. The fixed inter-element spacing of the array is kept as 0.75λ. The radiation patterns obtained with HPSO and SPSO are also shown in Fig. 10 (a) and (b), respectively. The proposed HPSOWM-based array has a reduced PSLL of –41.35 dB compared to –13.21 dB of isophoric 4D array. HPSOWM-based pulse splitting approach also produces low SBLs, and the first two SBLs are reported as –41.7 dB and –47.62 dB. The FNBW and directivity reported for the proposed 4D array are 11.88º and 13.72 dB compared to 9.72º and 13.80 dB of the isophoric array, respectively. The WM method exhibits superiority over the HPSO and SPSO methods as –32.34 dB and –32.70 dB PSLLs are obtained against –41.35 dB. The power generated at the central beam and first ten higher-order harmonics is presented in Fig. 11 (a). In addition to that, the first twenty higher SBLs are also reported in Fig. 11 (b) shows that the objective of SLL and SBLs reduction are achieved simultaneously with the proposed 4D arrays. In the proposed beamforming array with HPSOWM, 70.16% power is utilized and 29.84% is wasted in higher-order harmonics compared to 63.38%, 36.62% and 52.43%, 47.57% obtained with HPSO and SPSO, respectively. The optimal numerical outcomes are shown in Table 1.

4.1.3. Beamforming with 30-Element Array

The 30-element beamforming 4D linear array is also proposed for the simultaneous SLL and SBLs reduction with pulse splitting. The optimal results are targeted by optimizing the ON-time and the pulse splitting instants of each antenna element using HPSOWM. The HPSOWM-based outcomes are compared with HPSO-based, SPSO-based and uniform 4D arrays. The optimized beamforming switch schemes without and with pulse splitting derived by HPSOWM are presented in Fig. 12 (a) and (b). The radiation pattern for point-to-point beamforming array is given in Fig. 13. The fixed inter-element spacing of the array is kept as 0.75λ. The radiation patterns obtained with HPSO and SPSO are also shown in Fig. 14 (a) and (b), respectively. The proposed HPSOWM-based array has a reduced PSLL of –42.43 dB compared to –13.24 dB of isophoric 4D array. HPSOWM-based pulse splitting approach also produces low SBLs and the first two SBLs are reported as –42.14 dB and –44.15 dB. The FNBW and directivity reported for the proposed 4D array are 9.72º and 14.91 dB compared to 7.56º and 14.77 dB of the isophoric array, respectively. The WM method exhibits superiority over the HPSO and SPSO methods as –30.17 dB and –25.83 dB PSLLs are obtained against –42.43 dB. The power generated at the central beam and first ten higher-order harmonics is presented in Fig. 15 (a). In addition to that, the first twenty higher SBLs are also reported in Fig. 15 (b) shows that the objective of SLL and SBLs reduction are achieved simultaneously with the proposed 4D arrays. In the proposed beamforming array with HPSOWM, 71.96% power is utilized and 28.04% is dissipated in higher-order harmonics compared to 63.54%, 36.46% and 61.96%, 28.04% obtained with HPSO and SPSO, respectively. The optimal numerical outcomes are shown in Table 1.

4.2. Statistical Test and Comparison

To confirm the superiority of the WM method over HPSO and SPSO, two independents statistical t_test analysis is performed for the optimization problem in hand. Assuming unequal variances or standard deviations ($\sigma_1^2 \neq \sigma_2^2$) for a population, the test statistics may be calculated as [44]

$$t_{test} = \frac{\overline{\alpha}_{22} - \overline{\alpha}_{11}}{\sqrt{\left(\frac{\sigma_1^2}{n_A}\right) + \left(\frac{\sigma_2^2}{n_B}\right)}} \tag{28}$$

The degree of freedom (DoF) may be calculated as [44]

$$\beta = \frac{\left(\frac{\sigma_1^2}{n_A} + \frac{\sigma_2^2}{n_B}\right)^2}{\left\{\frac{\left(\frac{\sigma_1^2}{n_A}\right)^2}{(n_A - 1)} + \frac{\left(\frac{\sigma_2^2}{n_B}\right)^2}{(n_B - 1)}\right\}} \tag{29}$$

where, $\bar{\alpha}_{11}$ and $\bar{\alpha}_{22}$ are the means; σ_1 and σ_2 are the standard deviations; and n_A, n_B are the number of sample sizes considered for comparing the proposed algorithm with others. By considering $n_A = n_B$ for the 16-element 4D linear array, the t_test values obtained for different DoFs (β) comparing HPSOWM with HPSO and SPSO are presented in Table 2. The t_test values obtained are greater than the critical value [44], and that ensures the existence of an indicative deviation in HPSOWM's performance over HPSO and SPSO with 99.9% confidence.

The convergence plots of each method for the proposed 16, 24, and 30-element 4D linear arrays are shown in Fig. 16 (a), (b), and (c), respectively. A comparison of used and wasted power for the HPSOWM-based proposed arrays is reported in Fig. 16 (d). Comparison of efficiencies of the proposed arrays with execution time and optimized cost function values are reported in Table 3. Apart from all these statistical comparisons, the proposed array is also compared with other state of the art results, and presented in Table 4. The WM-based results show better performance in terms of array radiation properties compared to all the already reported works. Hence, a conclusion can be drawn that the proposed method is very well-suited for high-directive, secure point-to-point communication systems.

5. Conclusion

The adaptive radiation characteristics of fourth-dimensional (4D) linear antenna arrays have been explored in this article for beamforming applications. The point-to-point wireless communication system requires efficient, well-controlled, and optimized radiations patterns in specific directions. The proposed 4D array has achieved the target of getting ultra-low sidelobes beneficial for highly directive wireless transmission and reception. The optimality of the array has further enhanced by introducing a hybrid particle swarm optimizer with wavelet-based mutation approach. The optimal switching sequences have been derived for three sets of linear 4D arrays by considering the target

sidelobe below –40 dB. The inherent limitation of time-modulation, i.e., the formation of sidelobes at the multiple of harmonic frequencies have also been taken care of by proposing efficient pulse splitting techniques for all the arrays. The detailed comparison of the proposed array with simple PSO and hybrid PSO-based 4D arrays have also been reported which shows the effectiveness of the newly adopted mutation technique inspired by Morlet wavelets. Furthermore, the investigation of other reported works in this domain have also been carried over to compare the proposed array antenna. Finally, it can be concluded that all the three sets of arrays with reduced sidelobes and sidebands are applicable for directive wireless signal transmission or reception, and can further be explored in near future for more advanced applications.

Data Availability Statement

No new data were created or analyzed during this study. Data sharing is not applicable to this article.

Conflicts of Interests

The authors declare that they have no known competing financial interests or personal relationships that could have appeared to influence the work reported in this paper.

References

1. Rocca, P., Yang, F., Poli, L., et al., "Time-modulated array antennas–theory, techniques, and applications", *J. Electromagn. Waves Appl.*, **33**(12), pp. 1503–1531 (2019). doi: 10.1080/09205071.2019.1627251.

2. Shanks, H. E. and Bickmore, R. W., "Four-Dimensional Electromagnetic Radiators", *Can. J. Phys.*, **37**(3), pp. 263–275 (1959). doi: 10.1139/p59-031.

3. Shanks, H. E., "A New Technique for Electronic Scanning", *IRE Trans. Antennas Propag.*, **9**(2), pp. 162–166 (1961). doi: 10.1109/TAP.1961.1144965.

4. Kummer, W. H., Villeneuve, A. T., Fong, T. S., et al., "Ultra-Low Sidelobes from Time-Modulated Arrays", *IEEE Trans. Antennas Propag.*, **11**(6), pp. 633–639 (1963). doi: 10.1109/TAP.1963.1138102.

5. Brégains, J. C., Fondevila-Gómez, J., Franceschetti, G., et al., "Signal radiation and power losses of time-modulated arrays", *IEEE Trans. Antennas Propag.*, **56**(6), pp. 1799–1804 (2008). doi: 10.1109/TAP.2008.923345.

6. Yang, S., Gan, Y. B., and Qing, A., "Sideband suppression in time-modulated linear arrays by the differential evolution algorithm", *IEEE Antennas Wirel. Propag. Lett.*, **1**, pp. 173–175 (2002). doi: 10.1109/LAWP.2002.807789.

7. Poli, L., Rocca, P., Manica, L., et al., "Handling sideband radiations in time-modulated arrays through particle swarm optimization", *IEEE Trans. Antennas Propag.*, **58**(4), pp. 1408–1411 (2010). doi: 10.1109/TAP.2010.2041165.

8. Zhu, Q., Yang, S., Zheng, L., et al., "Design of a low sidelobe time modulated linear array with uniform

amplitude and sub-sectional optimized time steps", *IEEE Trans. Antennas Propag.*, **60**(9), pp. 4436–4439 (2012). doi: 10.1109/TAP.2012.2207082.

9. Chakraborty, A., Ram, G., and Mandal, D., "Optimal Pulse Shifting in Timed Antenna Array for Simultaneous Reduction of Sidelobe and Sideband Level", *IEEE Access*, **8**, pp. 131063–131075 (2020). doi: 10.1109/ACCESS.2020.3010047.

10. Chakraborty, A., Ram, G., and Mandal, D., "Time-modulated linear array synthesis with optimal time schemes for the simultaneous suppression of sidelobe and sidebands", *Int. J. Microw. Wirel. Technol.*, **14**(6), pp. 768–780 (2022). doi: 10.1017/S175907872100088X.

11. Tennant, A. and Chambers, B., "A two-element time-modulated array with direction-finding properties", *IEEE Antennas Wirel. Propag. Lett.*, **6**, pp. 64–65 (2007). doi: 10.1109/LAWP.2007.891953.

12. Li, G., Yang, S., Chen, Y., et al., "A novel electronic beam steering technique in time modulated antenna arrays", *Prog. Electromagn. Res.*, **97**, pp. 391–405 (2009). doi: 10.2528/PIER09072602.

13. Li, G., Yang, S., and Nie, Z., "Direction of arrival estimation in time modulated linear arrays with unidirectional phase center motion", *IEEE Trans. Antennas Propag.*, **58**(4), pp. 1105–1111 (2010). doi: 10.1109/TAP.2010.2041313.

14. Poli, L., Rocca, P., Oliveri, G., et al., "Harmonic beamforming in time-modulated linear arrays", *IEEE Trans. Antennas Propag.*, **59**(7), pp. 2538–2545 (2011). doi: 10.1109/TAP.2011.2152323.

15. Chakraborty, A., Ram, G., and Mandal, D., " Phase center motion based time modulated arrays with preprocessed time schemes for selective harmonic beamforming in B5G communication systems ", *Trans. Emerg. Telecommun. Technol.* (2023). doi: 10.1002/ett.4754.

16. Chakraborty, A., Ram, G., and Mandal, D., "Power pattern synthesis of a moving phase center time modulated antenna array using symmetrically and asymmetrically positioned time schemes", *Int. J. RF Microw. Comput. Eng.*, **32**(12) (2022). doi: 10.1002/mmce.23442.

17. Poli, L., Rocca, P., Manica, L., et al., "Pattern synthesis in time-modulated linear arrays through pulse shifting", *IET Microwaves, Antennas Propag.*, **4**(9), pp. 1157–1164 (2010). doi: 10.1049/iet-map.2009.0042.

18. Poli, L., Moriyama, T., and Rocca, P., "Pulse splitting for harmonic beamforming in time-modulated linear arrays", *Int. J. Antennas Propag.*, **2014** (2014). doi: 10.1155/2014/797590.

19. Poddar, S., Paul, P., Chakraborty, A., et al., "Design optimization of linear arrays and time-modulated antenna arrays using meta-heuristics approach", *Int. J. Numer. Model. Electron. Networks, Devices Fields*, **35**(5) (2022). doi: 10.1002/jnm.3010.

20. Chakraborty, A., Ram, G., and Mandal, D., "Pattern synthesis of timed antenna array with the exploitation and suppression of harmonic radiation", *Int. J. Commun. Syst.*, **34**(4) (2021). doi: 10.1002/dac.4727.

21. Chakraborty, A., Saxena, R. S., Verma, A., et al., "Multi-pattern synthesis in fourth-dimensional antenna arrays using BGM-based quasi-Newton memetic optimization method", *Int. J. Microw. Wirel. Technol.*, pp. 1–11 (2023). doi: 10.1017/S1759078723000910.

22. Chakraborty, A., Ram, G., and Mandal, D., "Time modulation based unconventional phased antenna arrays for monopulse and multifunction radar systems", *Int. J. Numer. Model. Electron. Networks, Devices Fields* (2022). doi: 10.1002/jnm.3074.

23. Tong, Y. and Tennant, A., "Simultaneous control of sidelobe level and harmonic beam steering in time-modulated linear arrays", *Electron. Lett.*, **46**(3), pp. 200–202 (2010). doi: 10.1049/el.2010.2629.

24. Chakraborty, A., Ram, G., and Mandal, D., "Multibeam steered pattern synthesis in time-modulated antenna array with controlled harmonic radiation", *Int. J. RF Microw. Comput. Eng.*, **31**(5) (2021). doi: 10.1002/mmce.22597.

25. Chakraborty, A., Ram, G., and Mandal, D., “Time-modulated multibeam steered antenna array synthesis with optimally designed switching sequence”, *Int. J. Commun. Syst.*, **34**(9) (2021). doi: 10.1002/dac.4828.

26. Chakraborty, A., Singh, I., Gupta, S., et al., “Sideband power control in Time-Modulated antenna arrays for bidirectional harmonic beamforming and beam scanning”, *AEU - Int. J. Electron. Commun.*, **170**, p. 154788 (2023). doi: 10.1016/j.aeue.2023.154788.

27. Maneiro-Catoira, R., Brégains, J., García-Naya, J. A., et al., “Dual-Beam Steerable TMAs Combining AM and PM Switched Time-Modulation”, *Sensors*, **22**(4) (2022). doi: 10.3390/s22041399.

28. Ram, G. and Mandal, D., “TMLAA for Automatic Harmonic Beam Steering Towards User Defined Direction Using Black Hole Mechanics Optimization”, *IEEE Trans. Cogn. Commun. Netw.* (2024). doi: 10.1109/TCCN.2024.3362325.

29. Ma, Y., Miao, C., Li, Y. H., et al., “A Partition-Based Method for Harmonic Beamforming of Time-Modulated Planar Array”, *IEEE Trans. Antennas Propag.*, **69**(4), pp. 2112–2121 (2021). doi: 10.1109/TAP.2020.3026893.

30. Li, H., Chen, Y., and Yang, S., “Directional Modulation in Time-Modulated Array with a Novel Pseudorandom Ascending Phase Time Sequence”, *IEEE Trans. Microw. Theory Tech.*, **70**(6), pp. 3319–3328 (2022). doi: 10.1109/TMTT.2022.3167693.

31. Dong, X., Li, H., Tan, J., et al., “A PSO-CVX Algorithm of Sum and Difference Beam Patterns for Time-Modulated Antenna Array”, *Int. J. Antennas Propag.*, **2021** (2021). doi: 10.1155/2021/6692872.

32. Chen, K., Yang, S., Chen, Y., et al., “Hybrid Directional Modulation and Beamforming for Physical Layer Security Improvement through 4-D Antenna Arrays”, *IEEE Trans. Antennas Propag.*, **69**(9), pp. 5903–5912 (2021). doi: 10.1109/TAP.2021.3060056.

33. Qu, C., Chen, K., Long, W., et al., “A Vector Modulation Approach for Secure Communications Based on 4-D Antenna Arrays”, *IEEE Trans. Antennas Propag.*, **70**(5), pp. 3723–3732 (2022). doi: 10.1109/TAP.2021.3137246.

34. Suneel Varma, D., Ram, G., and Arun Kumar, G., “Time-modulated multi-tone antenna array for wireless information and power transfer”, *Int. J. Commun. Syst.*, **36**(5) (2023). doi: 10.1002/dac.5419.

35. Ram, G., Kar, R., and Mandal, D., “Control parameter-based comparative study of radiation properties of TMCCAA and TMHSCAA”, *Sci. Iran.*, **29**(4), pp. 1939–1948 (2022). doi: 10.24200/sci.2020.53945.3503.

36. Varma, D. S., Ram, G., and Arun Kumar, G., “Time-Modulated Arrays: A Review”, *IETE Tech. Rev. (Institution Electron. Telecommun. Eng. India)*, **40**(1), pp. 136–151 (2023). doi: 10.1080/02564602.2022.2055669.

37. Del Ser, J., Osaba, E., Molina, D., et al., “Bio-inspired computation: Where we stand and what’s next”, *Swarm Evol. Comput.*, **48**, pp. 220–250 (2019). doi: 10.1016/j.swevo.2019.04.008.

38. Sharaqa, A. and Dib, N., “Design of Linear and Elliptical Antenna Arrays Using Biogeography Based Optimization”, *Arab. J. Sci. Eng.*, **39**(4), pp. 2929–2939 (2014). doi: 10.1007/s13369-013-0794-8.

39. Das, A., Mandal, D., Ghoshal, S. P., et al., “A Heuristic Approach to Design Linear and Circular Antenna Array for Side Lobe Reduction”, *Iran. J. Sci. Technol. - Trans. Electr. Eng.*, **43**, pp. 67–76 (2019). doi: 10.1007/s40998-018-0147-4.

40. Ram, G., Mandal, D., Kar, R., et al., “Improvement in various radiation characteristics of time modulated linear antenna arrays using evolutionary algorithms”, *J. Exp. Theor. Artif. Intell.*, **28**(1–2), pp. 151–180 (2016). doi: 10.1080/0952813X.2015.1020522.

41. Robinson, J. and Rahmat-Samii, Y., “Particle swarm optimization in electromagnetics”, *IEEE Trans. Antennas Propag.*, **52**(2), pp. 397–407 (2004). doi: 10.1109/TAP.2004.823969.

42. Ling, S. H., Iu, H. H. C., Chan, K. Y., et al., “Hybrid particle swarm optimization with wavelet mutation and its industrial applications”, *IEEE Trans. Syst. Man, Cybern. Part B Cybern.*, **38**(3), pp. 743–763 (2008). doi: 10.1109/TSMCB.2008.921005.

43. Weile, D. S. and Michielssen, E., “genetic algorithm optimization applied to electromagnetics: A review”, *IEEE Trans. Antennas Propag.*, **45**(3), pp. 343–353 (1997). doi: 10.1109/8.558650.

44. Scott, J. F., Walpole, R. E., and Myers, R. H., “Probability and Statistics for Engineers and Scientists”, *Math. Gaz.*, **57**(400), p. 148 (1973). doi: 10.2307/3615376.

45. Yang, S., Gan, Y. B., Qing, A., et al., “Design of a uniform amplitude time modulated linear array with optimized time sequences”, *IEEE Trans. Antennas Propag.*, **53**(7), pp. 2337–2339 (2005). doi: 10.1109/TAP.2005.850765.

46. Chen, J., Liang, X., He, C., et al., “Instantaneous Gain Optimization in Time Modulated Array Using Reconfigurable Power Divide/Combiner”, *IEEE Antennas Wirel. Propag. Lett.*, **17**(4), pp. 530–533 (2018). doi: 10.1109/LAWP.2018.2795008.

47. Aksoy, E. and Afacan, E., “Sideband level suppression improvement via splitting pulses in time modulated arrays under static fundamental radiation”, *Prog. Electromagn. Res. Symp.*, pp. 364–367 (2011). doi: 10.13140/2.1.4820.7367.

48. Yang, S. W., Chen, Y. K., and Nie, Z. P., “Simulation of time modulated linear antenna arrays using the FDTD method”, *Prog. Electromagn. Res.*, **98**, pp. 175–190 (2009). doi: 10.2528/PIER09092507.

49. Zhu, Q., Yang, S., Zheng, L., et al., “A pattern synthesis approach in four-dimensional antenna arrays with practical element models”, *J. Electromagn. Waves Appl.*, **25**(16), pp. 2274–2286 (2011). doi: 10.1163/156939311798147105.

50. He, C., Yu, H., Liang, X., et al., “Sideband radiation level suppression in time-modulated array by nonuniform period modulation”, *IEEE Antennas Wirel. Propag. Lett.*, **14**, pp. 606–609 (2015). doi: 10.1109/LAWP.2014.2373639.

List of Figures

List of Tables

Figures

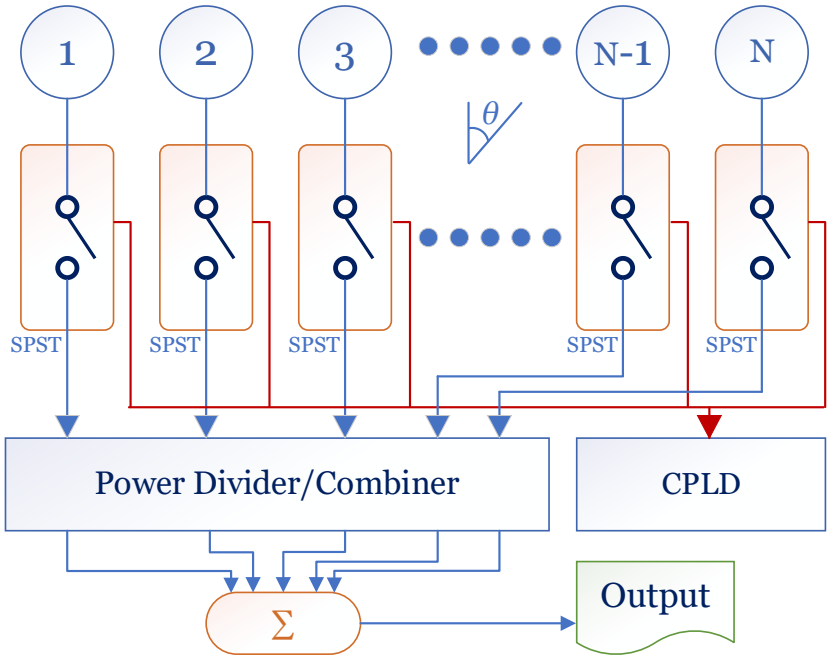

Figure 1. N-Element Fourth-Dimensional (4D) Linear Antenna Array with Beamforming Network (BFN)

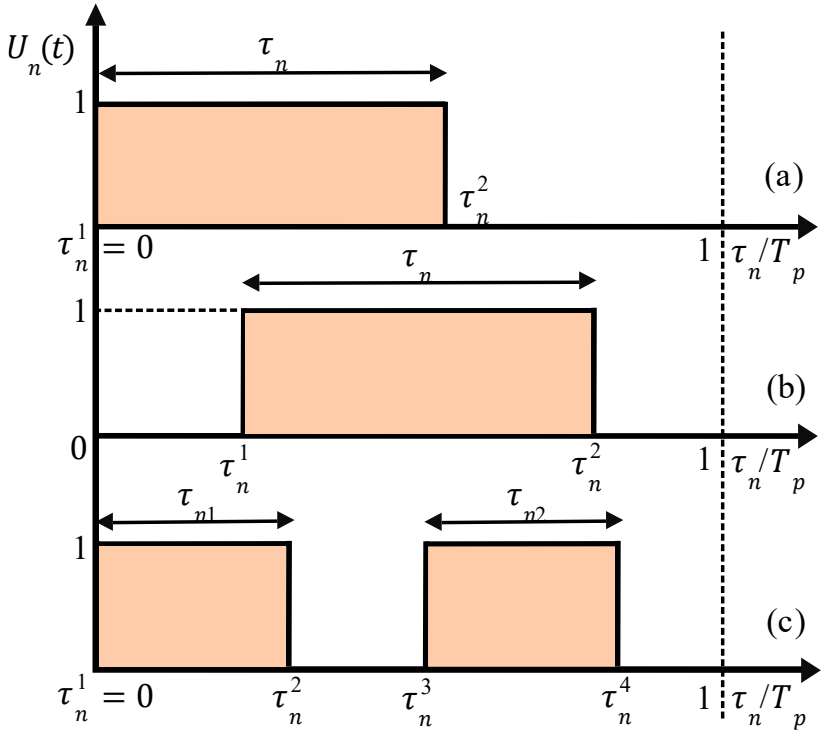

Figure 2. (a) Simple Pulse, (b) Shifted Pulse, (c) Sub-Sectioned Pulse (Pulse Splitting)

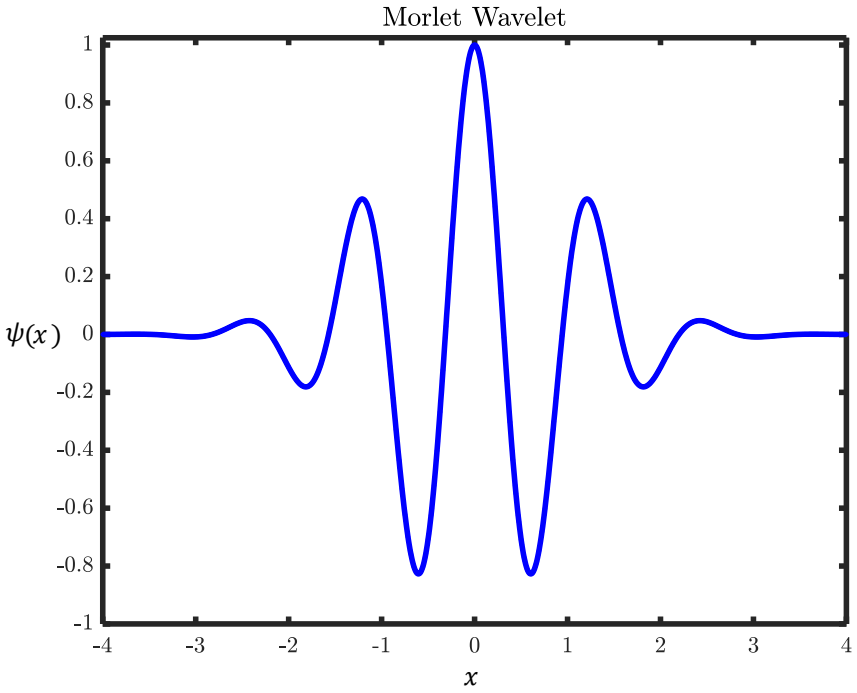

(a)

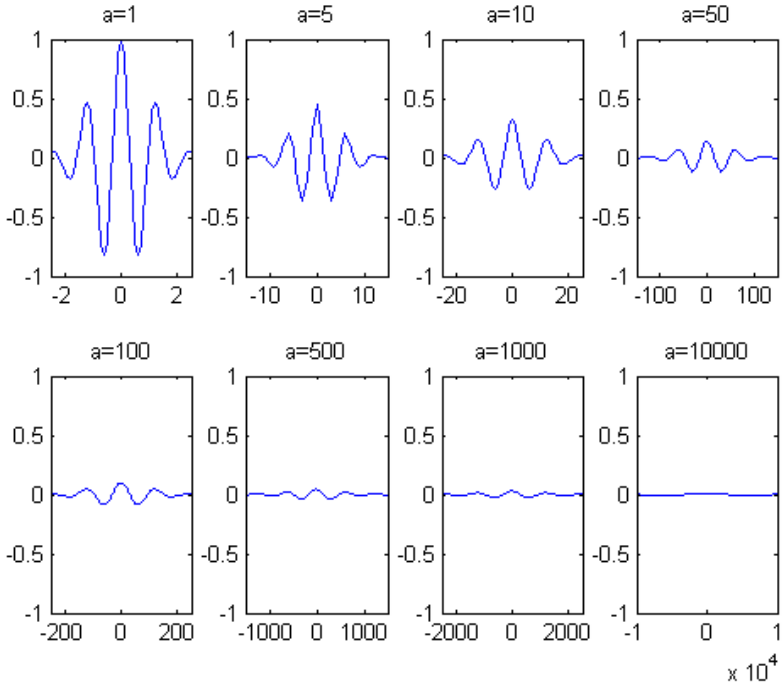

(b)

Figure 3. (a) Morlet Wavelet, (b) Characteristics of Morlet Wavelet for Different Dilating Parameter Values [42]

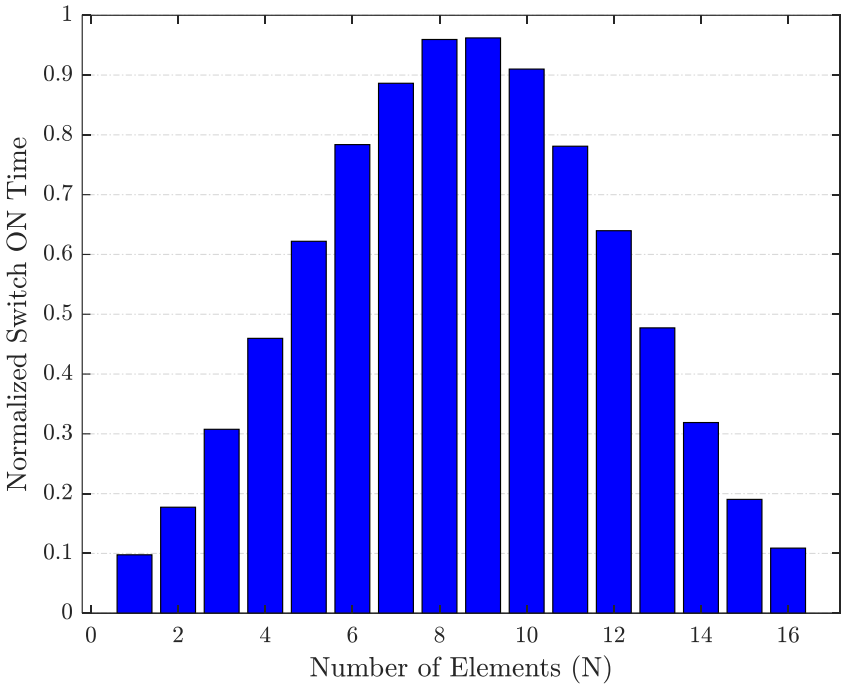

(a)

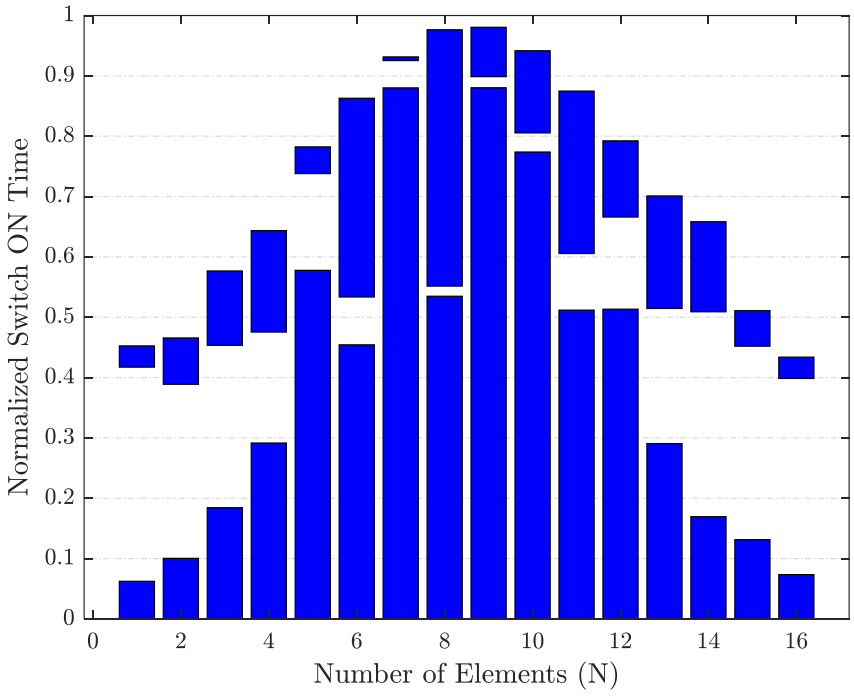

(b)

Figure 4. Optimal Beamforming Switch Schemes (a) Without and (b) With Pulse Splitting for 16-Element Array

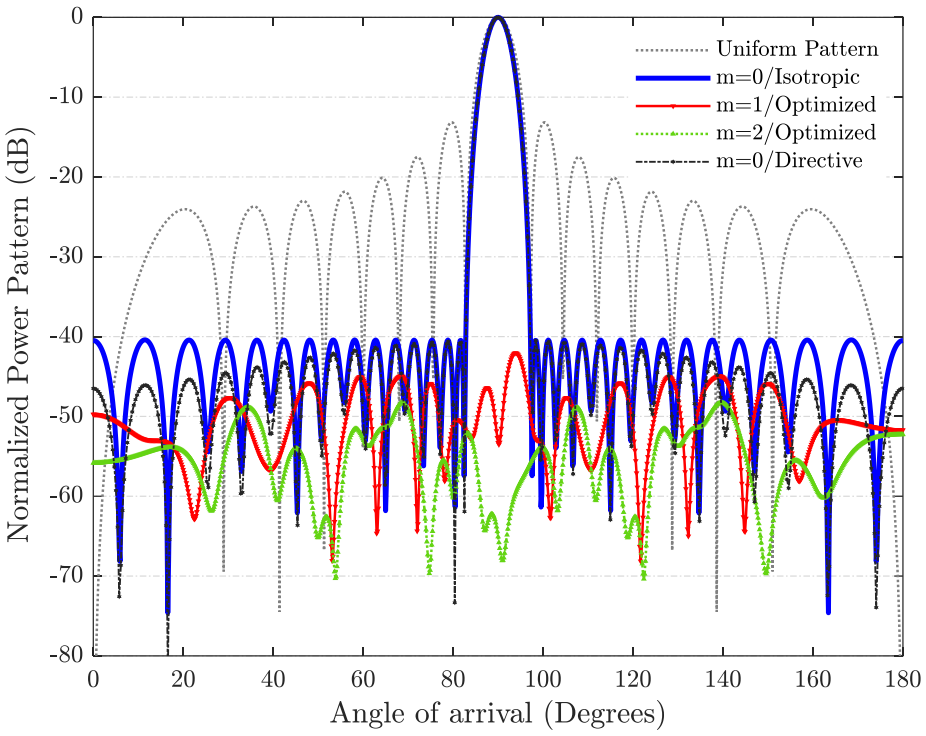

Figure 5. Optimal Beamforming Radiation Patterns with Reduced PSLL and SBLs for 16-Element Array

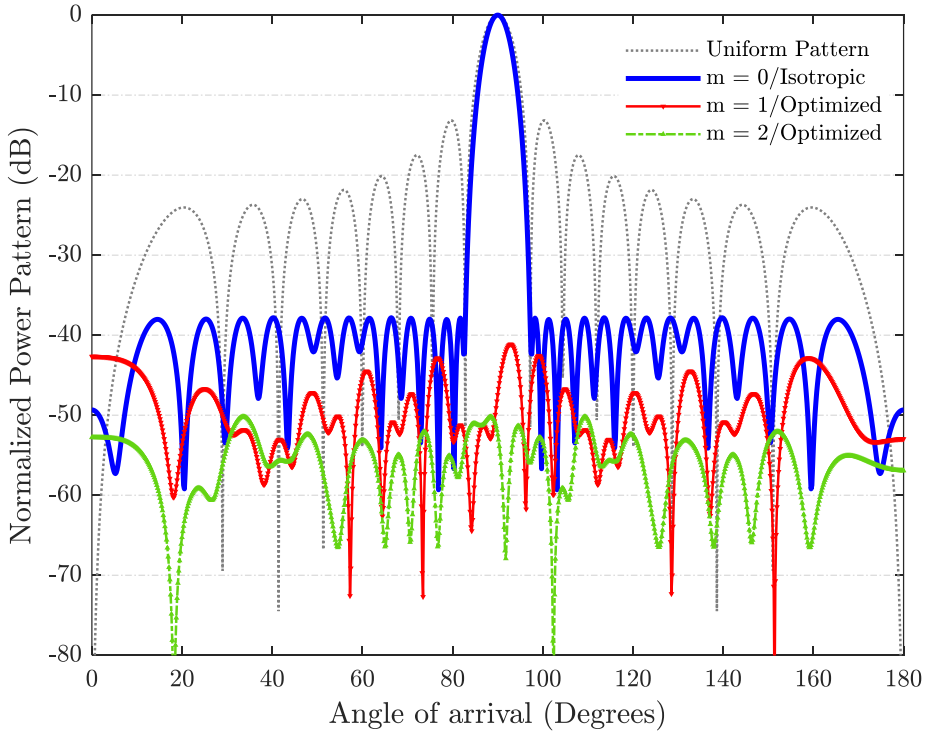

(a)

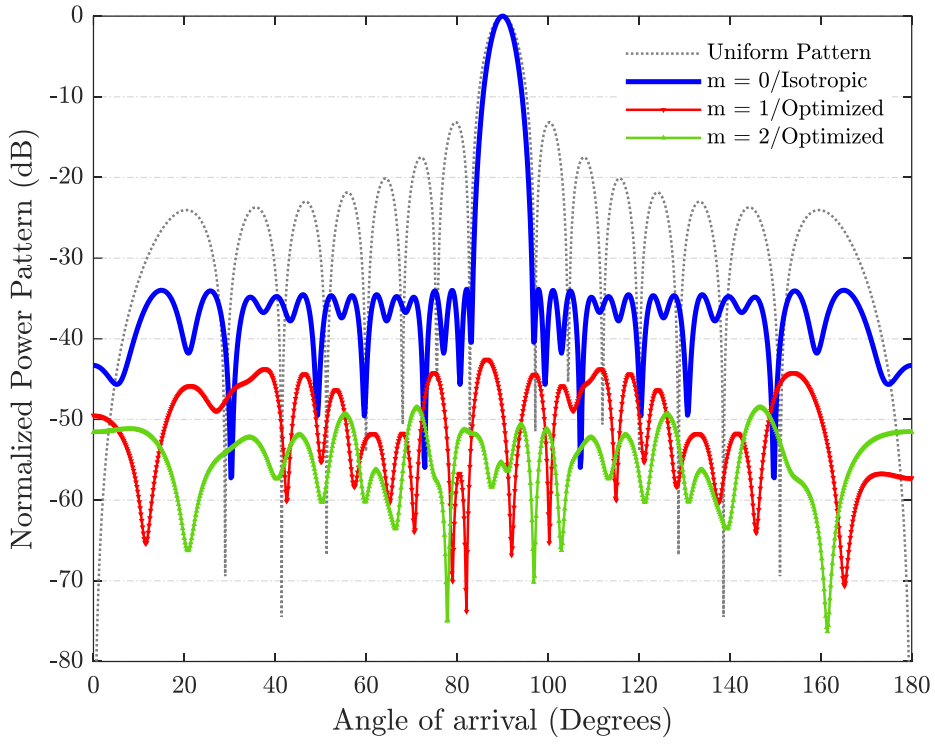

(b)

Figure 6. Beamforming Radiation Patterns 16-Element Array Using (a) HPSO and (b) SPSO-Based Schemes

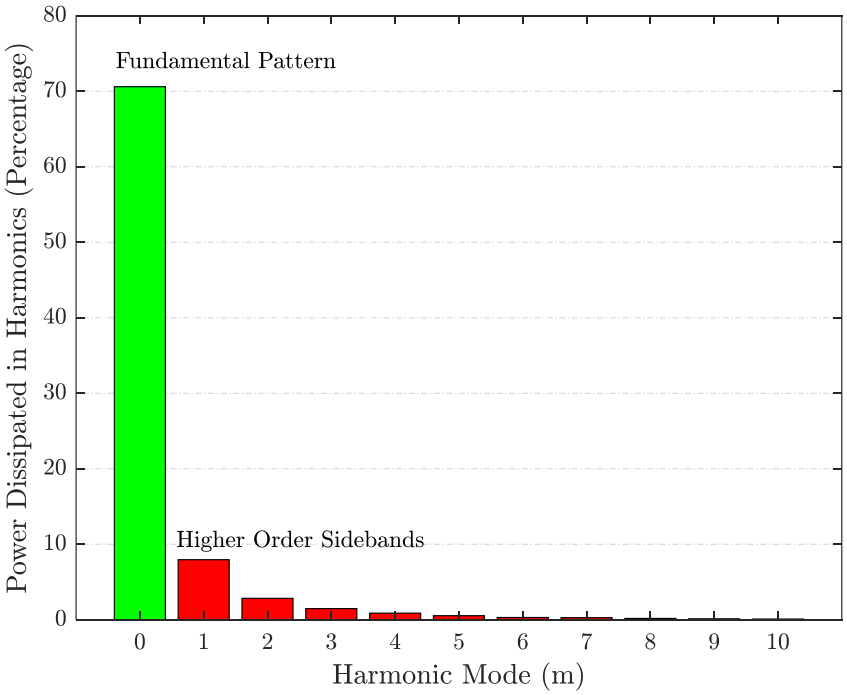

(a)

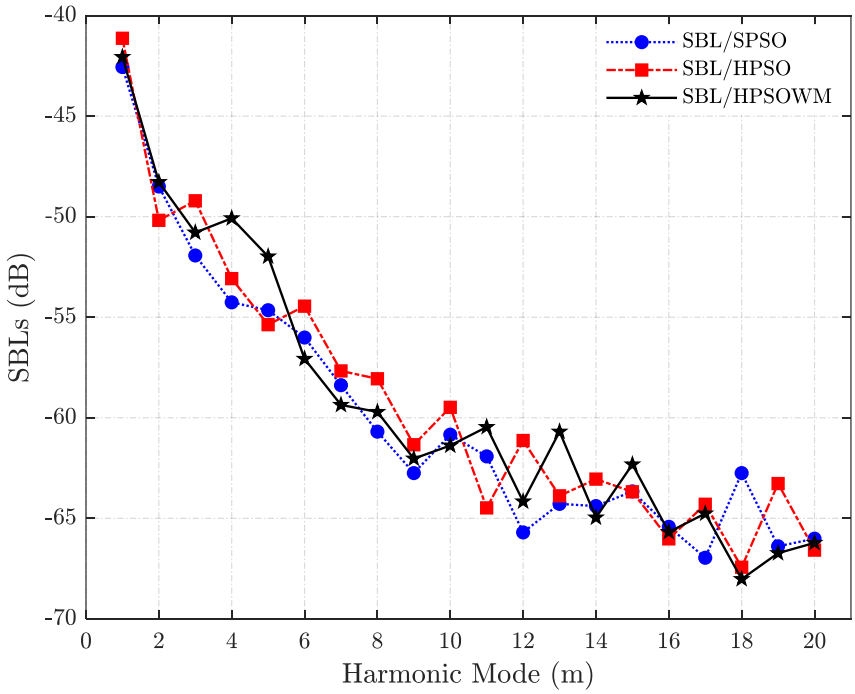

(b)

Figure 7. (a) Power Dissipated in Main Beam and Sidebands with HPSOWM, (b) Optimized Higher-Order SBLs

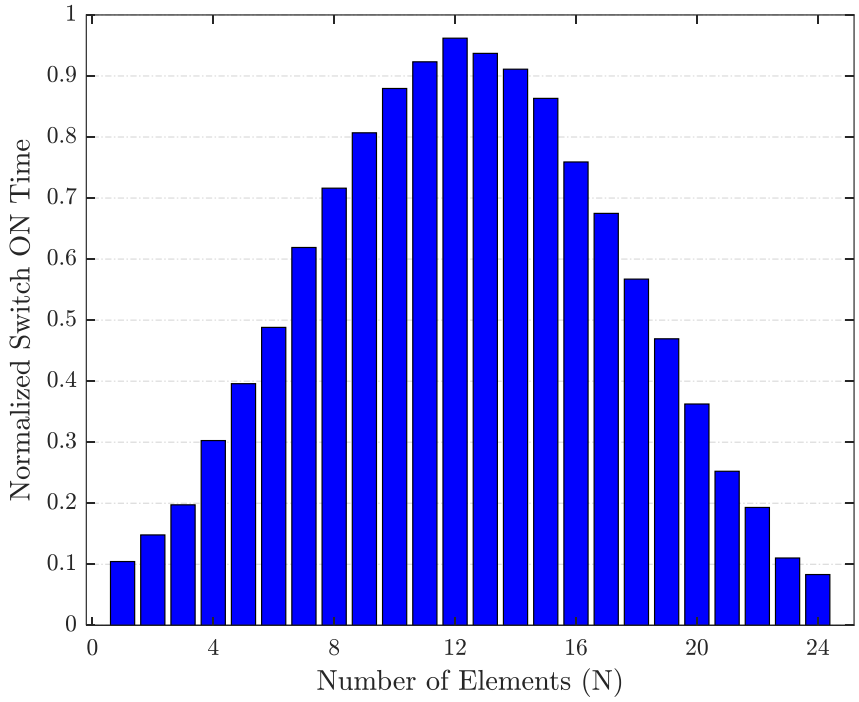

(a)

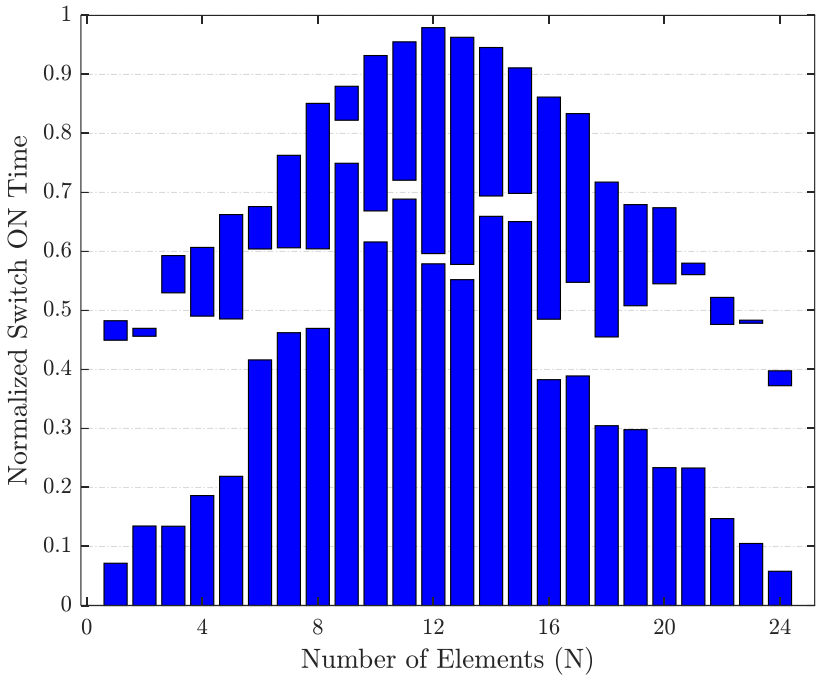

(b)

Figure 8. Optimal Beamforming Switch Schemes (a) Without and (b) With Pulse Splitting for 24-Element Array

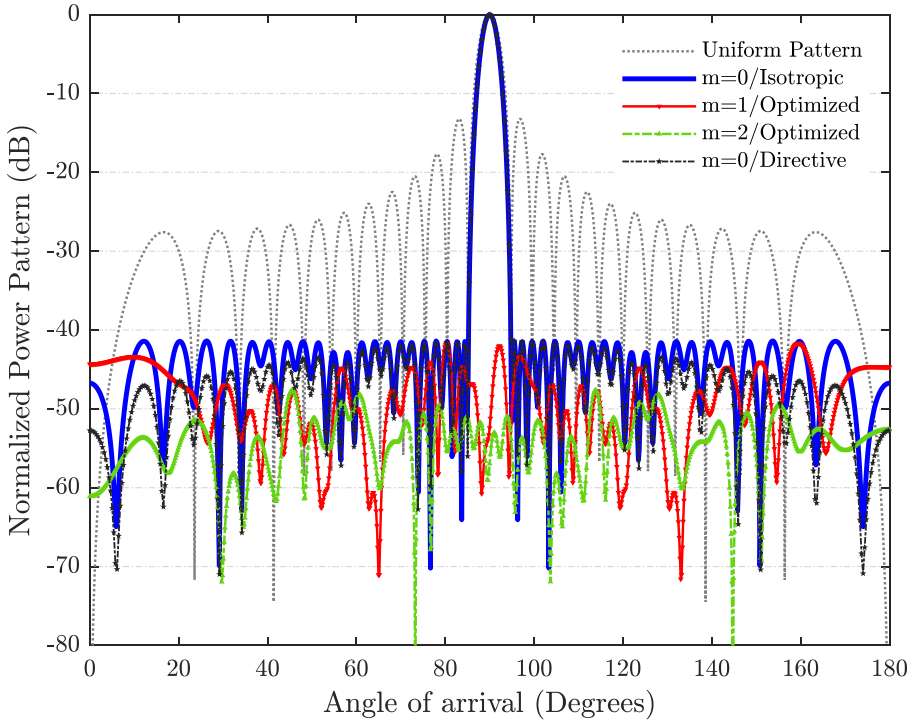

Figure 9. Optimal Beamforming Radiation Patterns with Reduced PSLL and SBLs for 24-Element Array

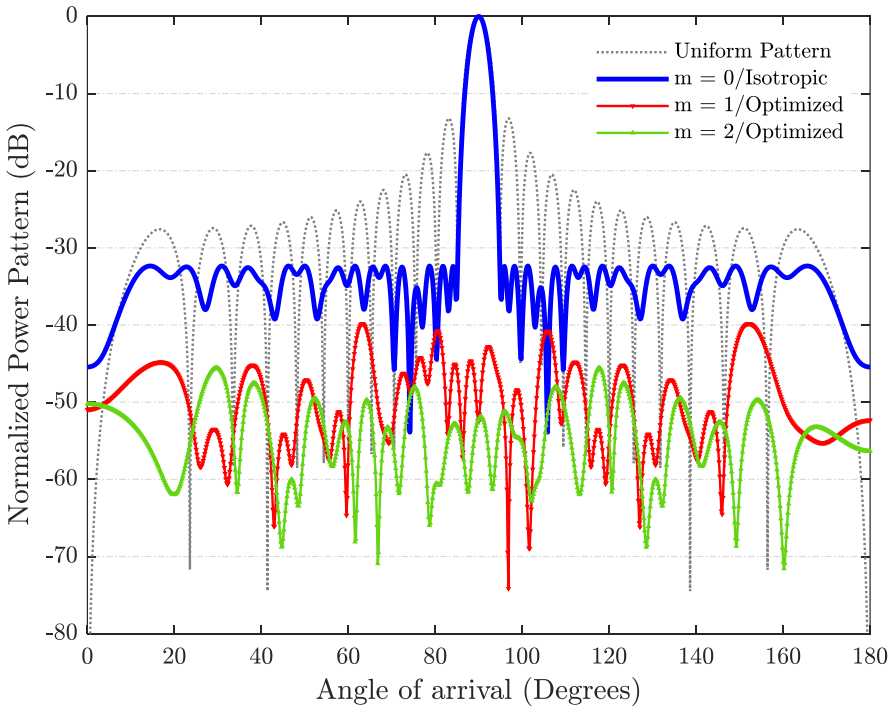

(a)

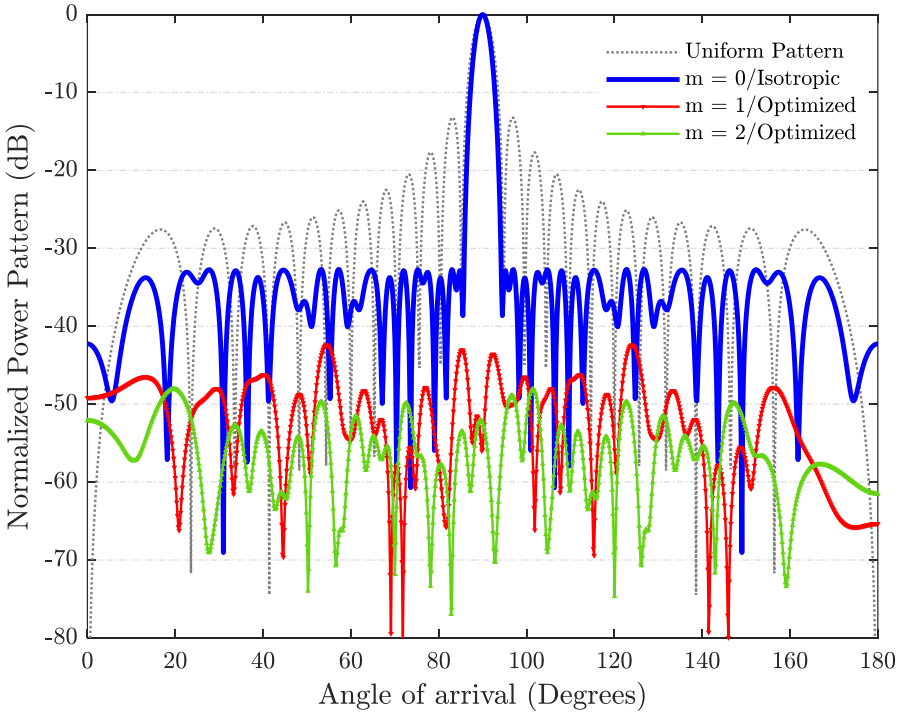

(b)

Figure 10. Beamforming Radiation Patterns 24-Element Array Using (a) HPSO and (b) SPSO-Based Schemes

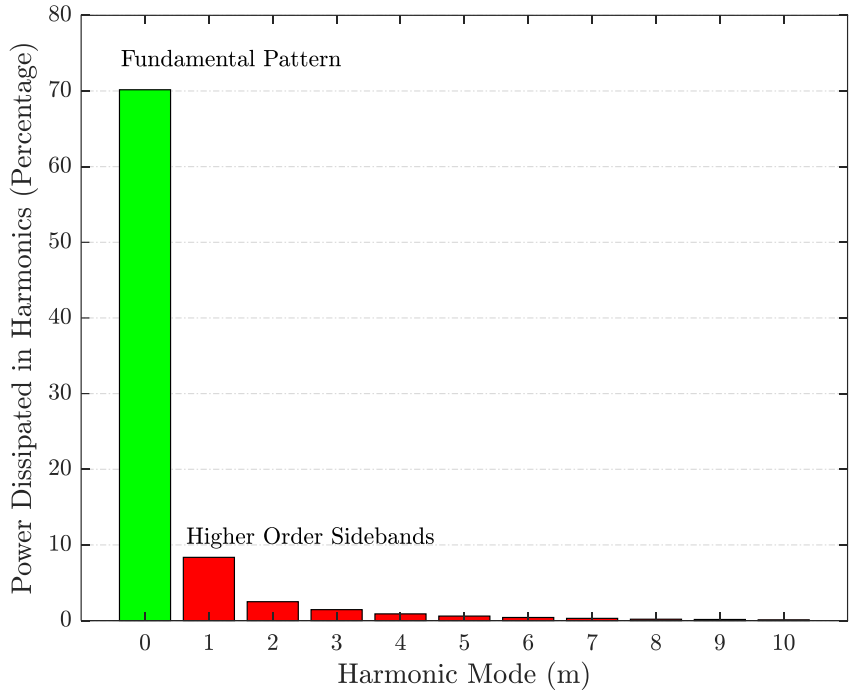

(a)

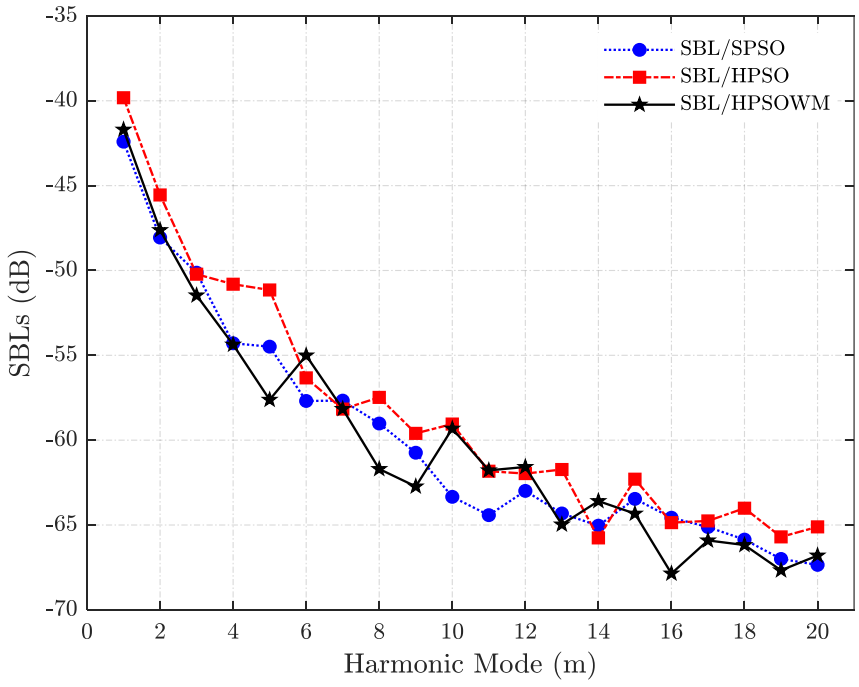

(b)

Figure 11. (a) Power Dissipated in Main Beam and Sidebands with HPSOWM, (b) Optimized Higher-Order SBLs

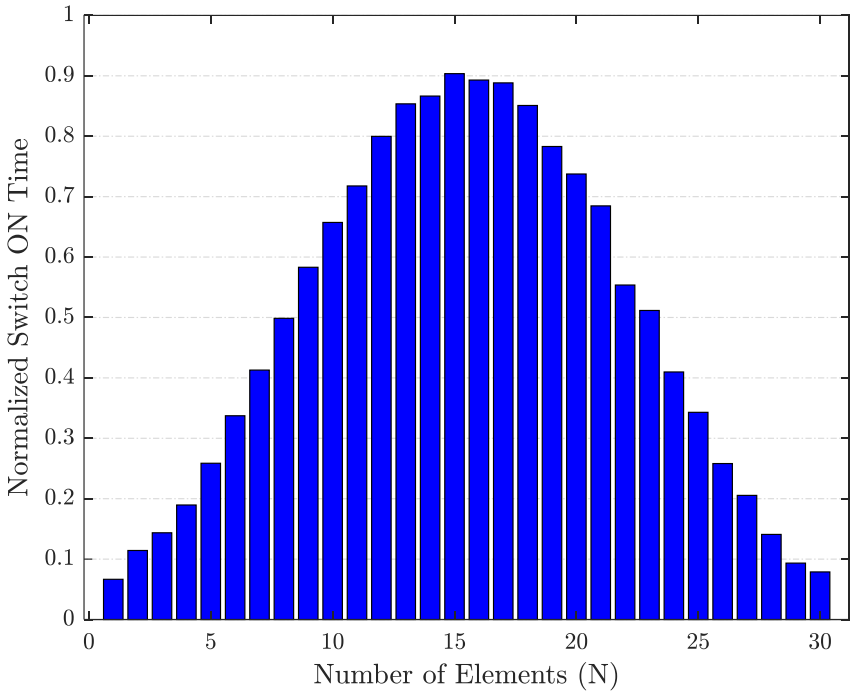

(a)

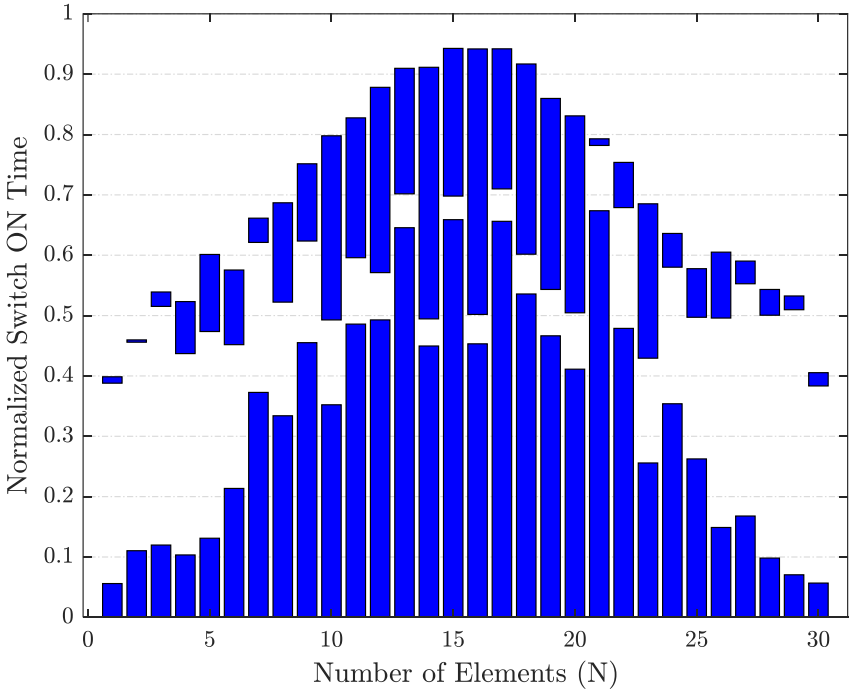

(b)

Figure 12. Optimal Beamforming Switch Schemes (a) Without and (b) With Pulse Splitting for 30-Element Array

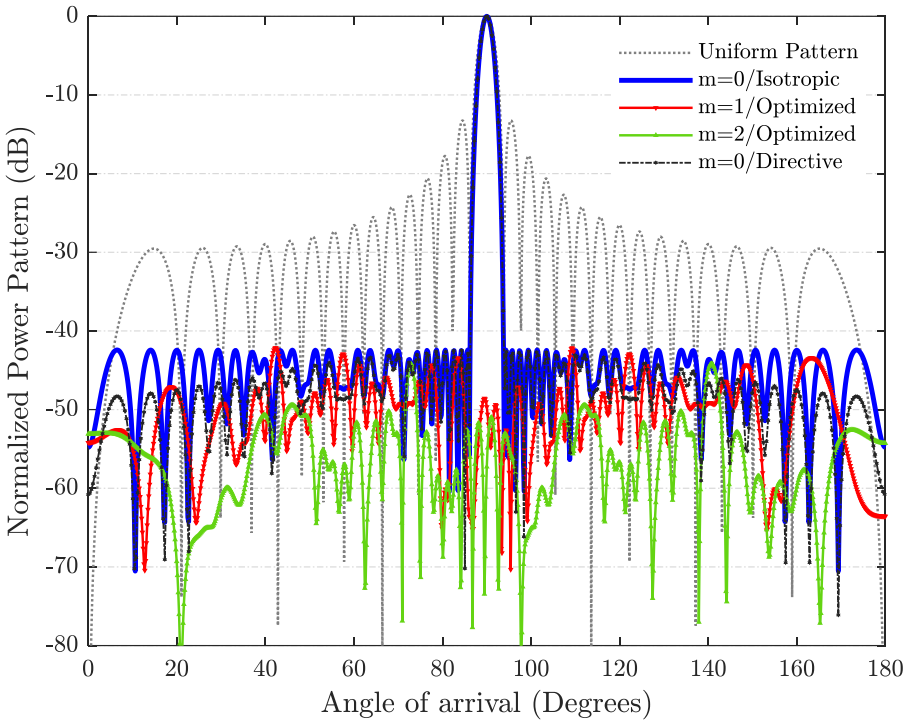

Figure 13. Optimal Beamforming Radiation Patterns with Reduced PSLL and SBLs for 30-Element Array

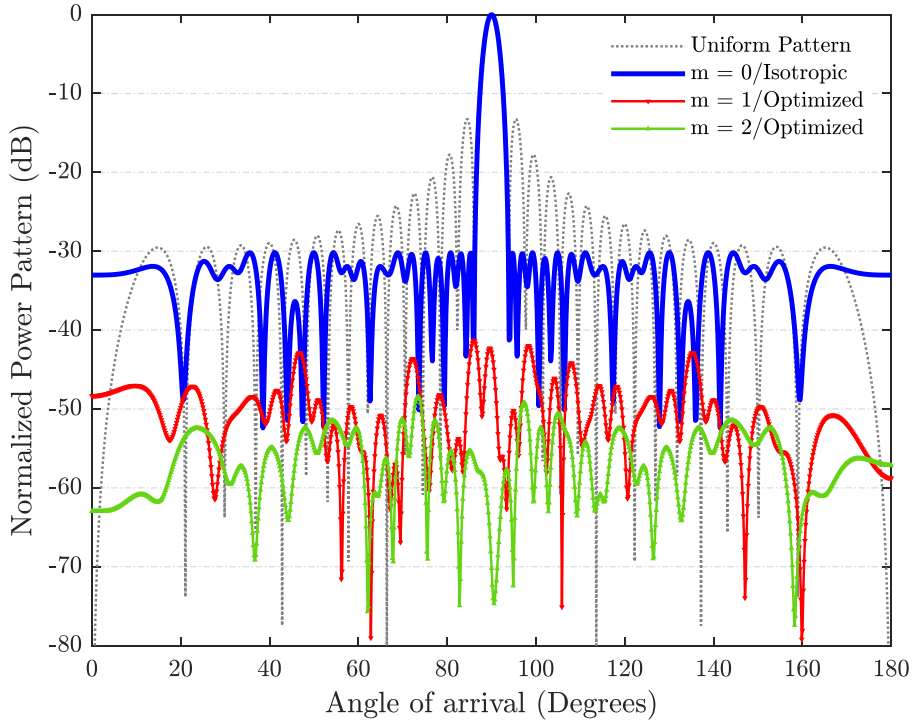

(a)

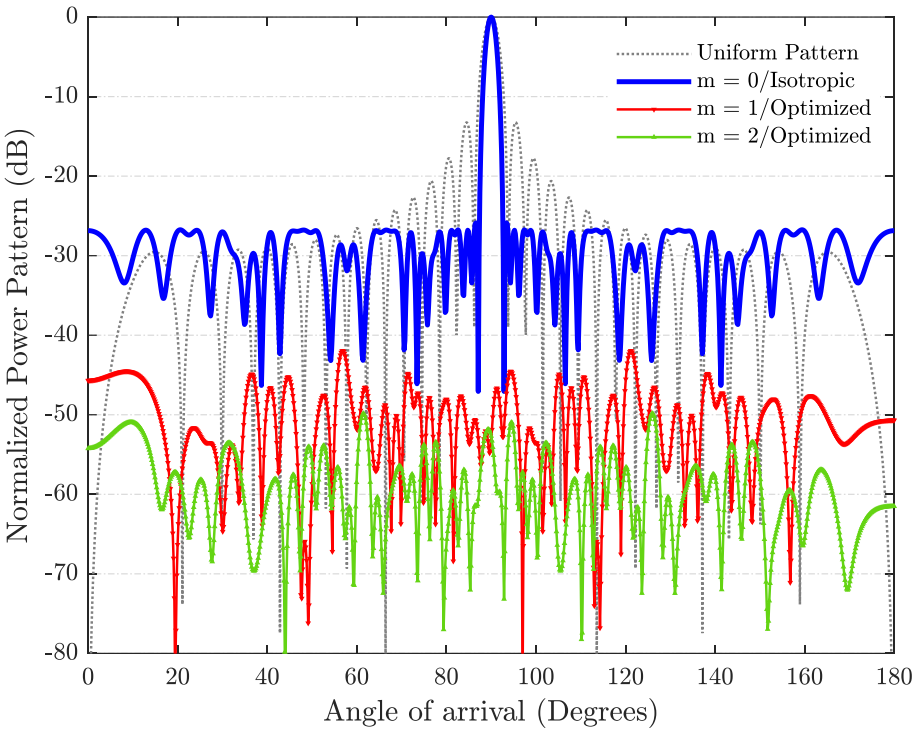

(b)

Figure 14. Beamforming Radiation Patterns 30-Element Array Using (a) HPSO and (b) SPSO-Based Schemes

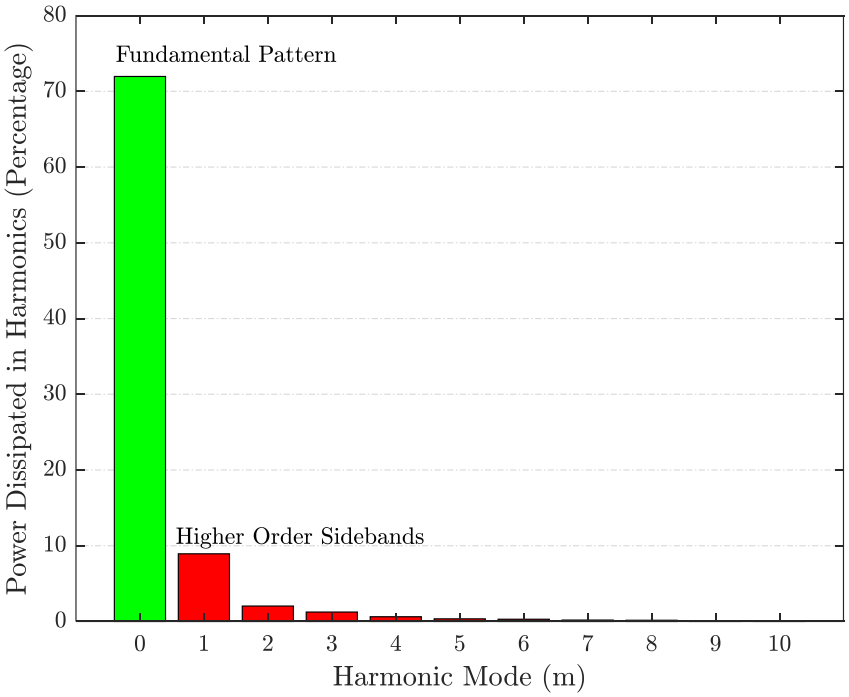

(a)

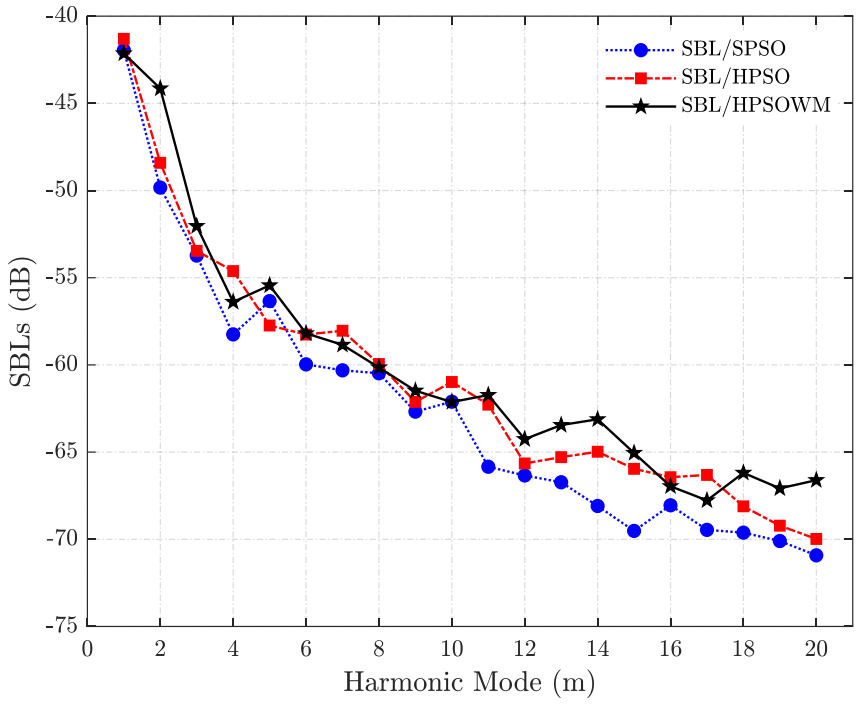

(b)

Figure 15. (a) Power Dissipated in Main Beam and Sidebands with HPSOWM, (b) Optimized Higher-Order SBLs

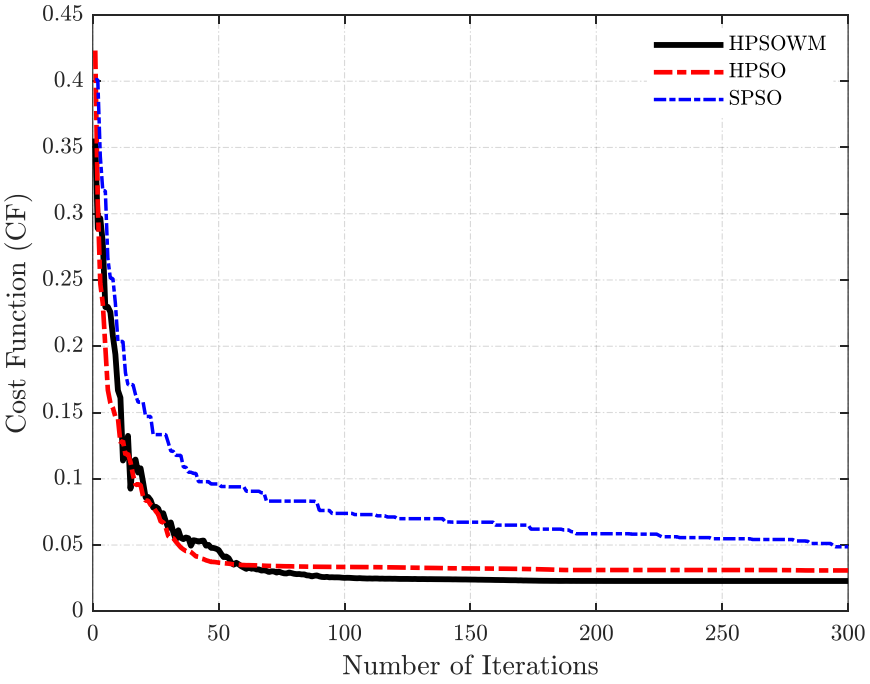

(a)

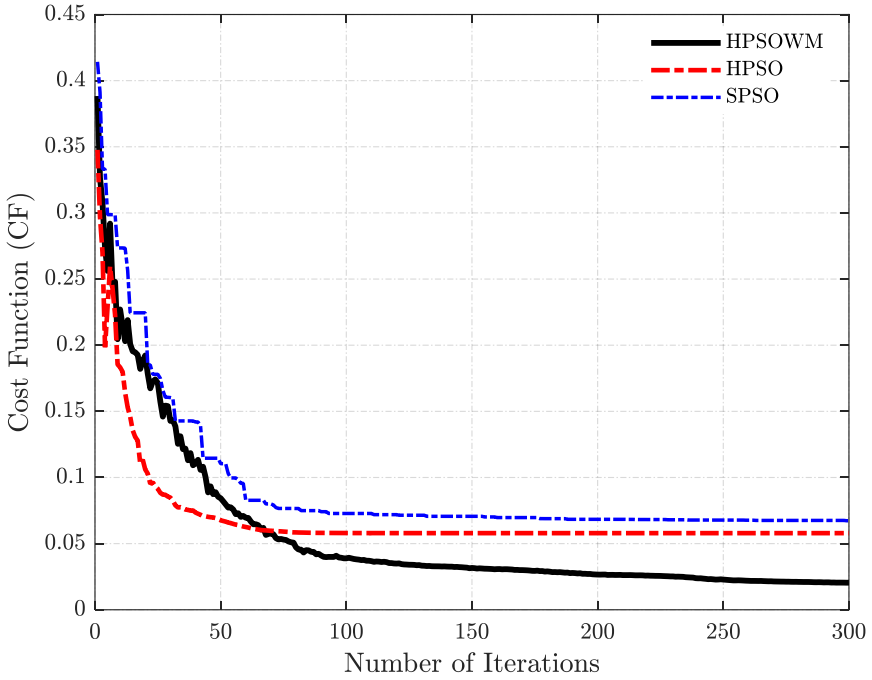
HPSOWM
HPSO
SPSO
Cost Function (CF)
Number of Iterations
0.45
0.4
0.35
0.3
0.25
0.2
0.15
0.1
0.05
0
0
50
100
150
200
250
300

(b)

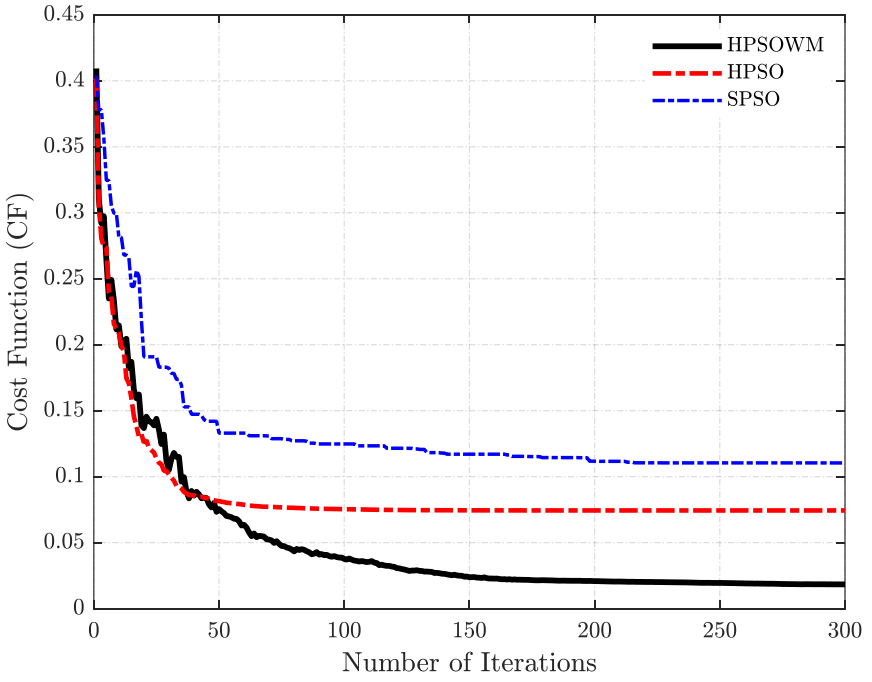
HPSOWM
HPSO
SPSO
Cost Function (CF)
Number of Iterations
0.45
0.4
0.35
0.3
0.25
0.2
0.15
0.1
0.05
0
0
50
100
150
200
250
300

(c)

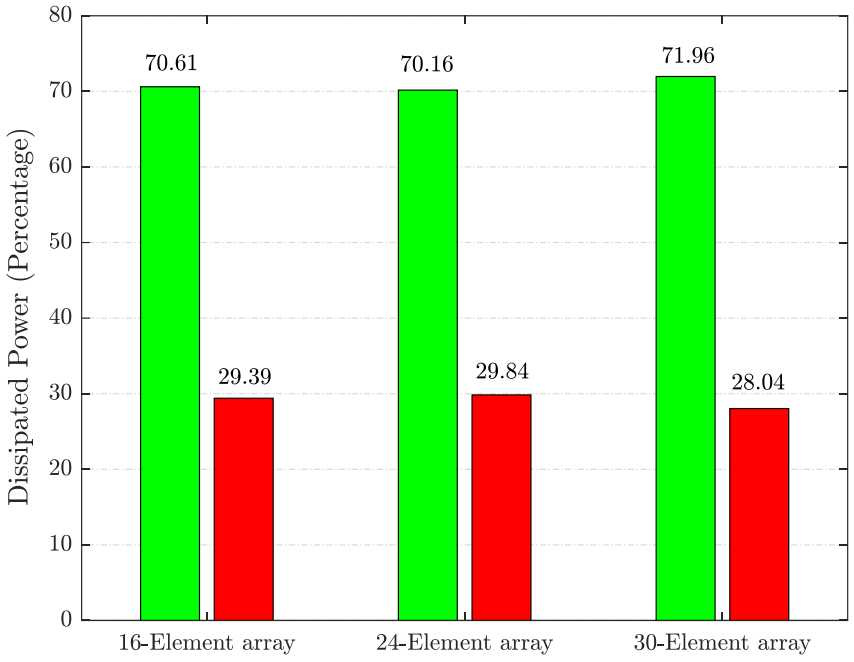

(d)

Figure 16. Convergence Plots for (a) 16-Element, (b) 24-Element, (c), 30-Element 4D array, and (d) Comparison of Used and Unused Power for HPSOWM-Based Proposed 4D arrays

Tables

Table 1. Numerical Results for the Proposed Beamforming 4D array with Optimized Time Schemes

Elements	Algorithms	ON-Time Durations (τ_n/T_p)			Pulse Splitting Instants (τ_n^r/T_p)			Spacing (λ)	PSLL$_0$ (dB)	PSBL$_1$ (dB)	PSBL$_2$ (dB)	FNBW ($degree$)	Directivity (dB)
16	**HPSOWM**	**0.0978**	**0.1774**	**0.3077**	**0.4174**	**0.3890**	**0.4536**	**0.75**	**-40.48**	**-42.60**	**-48.38**	**17.64**	**12.98**
		0.4598	**0.6221**	**0.7838**	**0.4755**	**0.7381**	**0.5336**						
		0.8864	**0.9596**	**0.9622**	**0.9254**	**0.5516**	**0.8987**						
		0.9101	**0.7811**	**0.6398**	**0.8055**	**0.6057**	**0.6661**						
		0.4773	**0.3190**	**0.1905**	**0.5146**	**0.5091**	**0.4521**						
			0.1090			**0.3986**							
	HPSO	0.1127	0.2018	0.3023	0.5223	0.4187	0.5024	0.75	-37.81	-41.13	-50.18	17.88	12.03
		0.4628	0.6057	0.7362	0.6672	0.4499	0.6423						
		0.8685	0.9246	0.9384	0.5767	0.7982	0.5706						
		0.8850	0.7937	0.6570	0.5729	0.5176	0.4708						
		0.4831	0.3510	0.1992	0.6556	0.5037	0.4773						
			0.1318			0.4208							
	SPSO	0.1727	0.2420	0.3678	0.4403	0.4131	0.4269	0.75	-33.89	-42.56	-48.50	17.84	12.02
		0.4766	0.6791	0.7723	0.5340	0.5342	0.5519						
		0.9053	0.9825	0.9313	0.6428	0.5854	0.5144						
		0.8966	0.8509	0.6679	0.6800	0.6071	0.6397						
		0.5470	0.3872	0.2400	0.5594	0.4044	0.5441						
			0.1443			0.3628							
24	**HPSOWM**	**0.1045**	**0.1481**	**0.1974**	**0.4496**	**0.4563**	**0.5299**	**0.75**	**-41.35**	**-41.7**	**-47.62**	**11.88**	**13.71**
		0.3027	**0.3959**	**0.4881**	**0.4904**	**0.4857**	**0.6042**						
		0.6190	**0.7162**	**0.8069**	**0.6062**	**0.6045**	**0.8224**						
		0.8795	**0.9232**	**0.9619**	**0.6688**	**0.7207**	**0.5964**						
		0.9370	**0.9111**	**0.8633**	**0.5779**	**0.6940**	**0.6984**						
		0.7591	**0.6749**	**0.5672**	**0.4852**	**0.5477**	**0.4551**						
		0.4694	**0.3626**	**0.2524**	**0.5079**	**0.5452**	**0.5607**						
		0.1931	**0.1103**	**0.0832**	**0.4763**	**0.4783**	**0.3725**						
	HPSO	0.1615	0.2337	0.2426	0.5044	0.4511	0.5174	0.75	-32.34	-39.82	-45.55	10.44	13.32
		0.3113	0.4240	0.4436	0.4684	0.5166	0.4952						
		0.5446	0.5605	0.6862	0.6830	0.5561	0.7773						
		0.6556	0.6701	0.7251	0.6752	0.5496	0.5583						
		0.6666	0.6276	0.6780	0.6296	0.5538	0.8223						
		0.5134	0.5006	0.4097	0.4921	0.5273	0.5249						
		0.3691	0.2764	0.2197	0.4296	0.4048	0.4370						
		0.1736	0.1115	0.1248	0.4907	0.4078	0.3795						

	SPSO	0.1420	0.1974	0.2981	0.4971	0.5566	0.4895	0.75	-32.70	-42.41	-48.06	10.44	13.26
		0.3374	0.5246	0.5058	0.5266	0.5470	0.5119						
		0.5965	0.7229	0.7457	0.6868	0.6352	0.7430						
		0.8321	0.8036	0.8340	0.5686	0.7241	0.5096						
		0.8546	0.8105	0.7627	0.9020	0.6562	0.7384						
		0.6905	0.5790	0.5727	0.4969	0.5960	0.5147						
		0.4235	0.3636	0.2482	0.5284	0.5141	0.4503						
		0.1688	0.1820	0.1671	0.4415	0.4081	0.4556						
30	**HPSOWM**	**0.0666**	**0.1143**	**0.1436**	**0.3880**	**0.4559**	**0.5151**	**0.75**	**-42.43**	**-42.14**	**-44.15**	**9.72**	**14.91**
		0.1896	**0.2587**	**0.3373**	**0.4370**	**0.4736**	**0.4517**						
		0.4129	**0.4986**	**0.5831**	**0.6212**	**0.5223**	**0.6235**						
		0.6573	**0.7177**	**0.7998**	**0.4928**	**0.5959**	**0.5712**						
		0.8536	**0.8665**	**0.9036**	**0.7017**	**0.4945**	**0.6980**						
		0.8930	**0.8883**	**0.8509**	**0.5019**	**0.7099**	**0.6016**						
		0.7830	**0.7375**	**0.6847**	**0.5433**	**0.5047**	**0.7820**						
		0.5537	**0.5116**	**0.4098**	**0.6789**	**0.4294**	**0.5801**						
		0.3430	**0.2582**	**0.2055**	**0.4972**	**0.4960**	**0.5527**						
		0.1409	**0.0934**	**0.0788**	**0.5006**	**0.5097**	**0.3834**						
	HPSO	0.1118	0.2507	0.2702	0.3818	0.4855	0.4958	0.75	-30.17	-41.3	-48.41	7.56	14.85
		0.3382	0.2861	0.4196	0.5099	0.5687	0.4563						
		0.4548	0.5684	0.5555	0.4929	0.6229	0.5877						
		0.7032	0.7080	0.7286	0.6355	0.6977	0.5296						
		0.8805	0.8695	0.8160	0.5070	0.5915	0.7109						
		0.8020	0.8807	0.7599	0.5708	0.6082	0.5036						
		0.7016	0.7439	0.7413	0.6116	0.4995	0.5748						
		0.6290	0.5314	0.5183	0.5726	0.6355	0.5284						
		0.5430	0.2878	0.2976	0.5524	0.5338	0.5228						
		0.2723	0.1613	0.2937	0.4842	0.4269	0.4196						
	SPSO	0.2080	0.3965	0.4622	0.5249	0.5267	0.5534	0.75	-25.83	-41.95	-49.83	7.20	14.20
		0.4419	0.6078	0.5646	0.4974	0.5264	0.6016						
		0.4850	0.5894	0.8703	0.5144	0.6551	0.4908						
		0.7703	0.8971	0.8449	0.5414	0.6153	0.5147						
		0.9364	0.8807	0.9989	0.7261	0.8876	0.8243						
		0.7851	0.9867	0.9659	0.5007	0.6267	0.9586						
		0.8659	0.9581	0.5878	0.6877	0.6929	0.6325						
		0.5423	0.8210	0.4419	0.6793	0.6707	0.5781						
		0.6046	0.4811	0.1926	0.5252	0.5302	0.3895						
		0.2991	0.2224	0.3029	0.5192	0.5763	0.5155						

Table 2. Statistical t_test Comparisons for the Proposed HPSOWM with HPSO and SPSO for 16-Element array

Comparing algorithms	***t_test* value**	**Degree of freedom (β)**	**Critical values of *t_test* for 99.99% Confidence Interval**
HPSOWM/HPSO	5.826570660454678	39	3.323
HPSOWM/SPSO	6.557087984054862	36	3.347

Table 3. Comparison of Efficiency of Proposed Array with Execution Time and Optimized Cost Function Values

Elements	Algorithms	Execution Time (Min)	Cost Function Value	Standard Deviation of CF	Array Efficiency (%)
16	**HPSOWM**	**2.4038**	**0.022859**	**0.03012**	**70.61**
	HPSO	2.9976	0.030835	0.05042	70.01
	SPSO	3.8972	0.048687	0.05732	68.72
24	**HPSOWM**	**3.1078**	**0.020461**	**0.02892**	**70.16**
	HPSO	4.5578	0.057925	0.05845	63.38
	SPSO	6.0985	0.067312	0.08764	52.43
30	**HPSOWM**	**4.1176**	**0.018379**	**0.02206**	**71.96**
	HPSO	6.0654	0.074395	0.09558	63.54
	SPSO	6.9895	0.110410	0.13167	61.96

Table 4. Comparison of the Proposed HPSOWM-Based Outcomes with Other Works for 16-Element array

References	$PSLL_0$ (*dB*)	$PSBL_1$ (*dB*)	$PSBL_2$ (*dB*)	Power Used (%)
Reference [8]	-30.00	-27.80	Na	Na
Reference [17]	-30.00	-19.50	-21.70	Na
Reference [45]	-25.50	-24.60	Na	Na
Reference [46]	-30.00	-25.53	-25.01	Na
Reference [47]	-30.00	-22.51	Na	Na
Reference [48]	-39.60	-29.90	Na	Na
Reference [49]	-31.90	-21.80	Na	Na
Reference [40]	-38.67	-24.98	-32.64	46.79
Reference [40]	-40.41	-24.96	-32.64	46.92
Reference [50]	-30.00	-35.98	Na	Na
Proposed (This work)	**-40.48**	**-42.60**	**-48.38**	**70.61**

Biographies

Avishek Chakraborty passed his B. Tech degree in Electronics and Communication Engineering. He received his M. Tech degree in Radio Physics and Electronics with a specialization in Space Science and Microwaves from the University of Calcutta, West Bengal, India, in 2017. He has completed his Ph.D. in Electronics and Communication Engineering from National Institute of Technology (NIT) Durgapur in 2021. He has also successfully completed a DST-SERB sponsored research project by serving as a DST-SERB Research Fellow in his Ph.D. tenure (2018-2021). He is presently working as an Assistant Professor at the Department of Electrical, Electronics & Communication Engineering (EECE), GST, GITAM University, Bangalore. Prior to this, he was associated with the Department of Electronics and Communication Engineering (ECE), School of Engineering (SoE), SR University Warangal, Telangana, India as Assistant Professor. He has authored several research papers published in peer reviewed International Journals, Conferences, and Book Chapters. He has also served as a reviewer of IEEE Access, International Journal of RF and Computer-Aided Engineering (Wiley), Circuits Systems and Signal Processing (Springer), The Journal of Supercomputing (Springer), etc. His current research interests include Antenna Array Synthesis, Phased Arrays, Antenna Array Optimization using Soft Computing and Artificial Intelligence, and Signal Processing for Antenna Arrays and Radars.

Ravi Shankar Saxena received his B.E. degree in Electronics and Communication Engineering from Rohilkhand University, India, in 2000. He has completed his M. Tech from MNNIT Allahabad in 2004, and D. Phil in Communication Technology from Department of Electronics and Communication, University of Allahabad in 2016. He has published more than 16 research papers in different national and international journals and conference proceedings. His areas of interests include Patch antenna, Experimental nanoscience including Nanostructure fabrication, Optoelectronics properties, and Energy technologies. He is currently working as a Professor in GMRIT, Razam, Andhra Pradesh, India.

Indrasen Singh is working as an Associate Professor in the Department of Electronics and Communication Engineering at SR University, Warangal, Telangana, India. He received his BTech and MTech Degree in electronics and communication engineering from Uttar Pradesh Technical University, Lucknow, India in 2006, and 2010, respectively. He obtained his PhD degree in electronics and communication engineering from National Institute of Technology Kurukshetra, Haryana, India in 2019. He has more than 12 years of teaching, research experience in various reputed technical institutes or universities. He is the editorial board member of AJECE, Science Publishing Group, USA. He is the reviewer of many international journals and served as TPC member and reviewer in different conferences. He has published more than 20 research papers in National/International journals/conferences of repute and many are under review. His research interests are in the area of cooperative communication, stochastic geometry, modeling of wireless networks, heterogeneous networks, millimeter wave communications, device-to-device, and 5G/6G communication.

Jyoti Bansal is an accomplished academic and researcher currently serving as a faculty member in the Department of Electronics and Communication Engineering at Chandigarh Engineering College, Jhanjeri, Punjab, India. With a strong academic background and a passion for research, she has made significant contributions to the field of electronics and communication engineering. Jyoti Bansal has published 10 research papers in reputable conferences and journals. Her research primarily focuses on power quality and optimization, fields that are critical for the efficient and reliable operation of modern electrical systems.

Alaa Salim Abdalrazzaq is a dedicated academic currently serving at Al-Noor University College, Iraq. He has made significant contributions to the field by publishing five papers in SCOPUS-indexed journals and proceedings. His active participation in numerous international conferences underscores his commitment to staying at the forefront of research and innovation. Alaa's research interests are diverse, focusing on optimization, cryptocurrency, and algorithm development, areas critical to advancing modern technology and digital finance.

Mustafa Asaad Rasol is working as an Assistant Professor at the National University of Science and Technology, Dhi Qar, Iraq. He is doing research and teaching for the last 4 years. He has published 9 in SCOPUS indexed journals. He has attended many conferences at the international level. His research interests include electric power components and systems.

Anita Gehlot is currently associated with Uttaranchal University as Professor & Head (Research & Innovation) with more than Fifteen years of experience in academics. She is among top ten innovators of decade 2010-2020 listed by Clarivate Analytics (WoS). She has more than 500 patents in her account including 145 Indian and international IPR grants.

Sandip Bhattacharya is presently working as an Associate Professor at Department of ECE, SR University, Warangal. He received his PhD degree in VLSI from the School of VLSI Technology, Indian Institute of Engineering Science and Technology (IIEST), Shibpur, Howrah, India in 2017. He completed his Post-Doctoral Research from HiSIM Research Centre, Hiroshima University, Japan. He has more than 13 years of teaching, research, and Industry experience. He has published more than 62 research articles in archival journals and refereed conference proceedings. He received IETE J.C Bose Memorial Award for the best paper in the year 2018 from IETE, New Delhi. He is serving as a reviewer in IET Micro-nano Letters, IET Circuit Device and Systems, Journal of Computational Electronics (JCEL) Springer, IEEE Access, IEEE Sensors, IEEE Transaction on VLSI, IEEE Transaction on Nano Technology, Scientific Report, International Journal of Numerical modelling: network, devices, and fields (Wiley) etc. His research interests include VLSI design, interconnect modelling using next generation nano material, implementation on 3D IC and memory devices and artificial intelligence-based circuit design for robotics application.

Kalyan Sundar Kola completed M. Tech in Telecommunication Engineering from the department of Electronics and Communication Engineering, National Institute of Technology Durgapur, West Bengal, India in 2014. He has received his PhD degree from National Institute of Technology Goa in 2022. Presently, he is associated as Associate Professor in the Department of CSE at Brainware University, Barasat, Kolkata. His research area includes microstrip fractal patch antenna, antenna with DGS structure, miniaturized antenna, array of fractal antennas, dual-band array antenna and shifted-beam antenna array. He has published 17 research papers in international journals and 16 papers in international conferences. He received Gandhian Young Technological Innovation (GYTI) appreciation award in 2019 and also 3 Best paper awards from IEEE International Conferences.

Gopi Ram passed B.E. Degree in Electronics and Telecommunication Engineering from Government Engineering College, Jagdalpur, Chhattisgarh, India in the year 2007. He received his M. Tech degree in Telecommunication Engineering from National Institute of Technology Durgapur, West Bengal, India in the year 2011. He joined as a full-time Institute Research Scholar in the year of 2012 at National Institute of Technology, Durgapur to carry out research for Ph.D. degree. He received the scholarship from the Ministry of Human Resource and Development (MHRD), Government of India for the period 2009-2011 (M. Tech) and 2012-2015 (Ph. D). He is currently working as an Assistant Professor at the Department of Electronics and Communication Engineering, National Institute of Technology, Warangal, Telangana, India. His research interests include Evolutionary Optimization Based Radiation Pattern Synthesis of Antenna Arrays, Time modulated antenna arrays, and Applications of soft computing techniques in electromagnetics. He has published more than 50 research papers in International Journals and Conferences.

Durbadal Mandal passed B.E. degree in Electronics and Communication Engineering from Regional Engineering College, Durgapur, West Bengal, India in the year 1996. He received M. Tech and Ph.D. degrees from National Institute of Technology, Durgapur, West Bengal, India in the year 2008 and 2011, respectively. Presently, he is attached with National Institute of Technology Durgapur, West Bengal, India, as Associate Professor in the Department of Electronics and Communication Engineering. He has supervised 16 doctoral students, and has completed 2 DST-SERB Sponsored Research Projects as Project Investigator till date. His research interest includes Array Antenna design; filter Optimization via Evolutionary Computing Techniques. He has published more than 350 research papers in International Journals and Conferences.